

Models and Information Rates for Multiuser Optical Fiber Channels with Nonlinearity and Dispersion

Hassan Ghozlan, *Member, IEEE*, and Gerhard Kramer, *Fellow, IEEE*

Abstract—Two discrete-time interference channel models are developed for information transmission over a single span of optical fiber using wavelength-division multiplexing (WDM) and lumped amplification. The models are derived from the nonlinear Schrödinger (NLS) equation by including the nonlinear phenomena of self-phase modulation (SPM) and cross-phase modulation (XPM) but ignoring four-wave mixing (FWM), polarization effects and group velocity dispersion (GVD) within WDM bands. The first model also ignores GVD across WDM bands, referred to as group velocity mismatch (GVM). For the case of two users, a new technique called *interference focusing* is proposed where each carrier achieves the capacity pre-log 1, thereby doubling the pre-log of 1/2 achieved by using conventional methods. For three users, interference focusing is also useful under certain conditions. The second model captures GVM and the effect of filtering at the receivers in addition to SPM and XPM. In a 3-user system, it is shown that all users can achieve the maximum pre-log factor 1 simultaneously by using interference focusing, a time-limited pulse and a bank of filters at the receivers.

Index Terms—Optical fiber, wavelength-division multiplexing, Kerr nonlinearity, cross-phase modulation, chromatic dispersion, group velocity mismatch, interference channel.

I. INTRODUCTION

THE majority of traffic in core networks is carried by optical fiber. Understanding the ultimate limits of communication over optical fiber is thus of great importance and would help to provide guidelines for designing networks. An appealing property of fiber is that it has low attenuation over a large range of frequencies which allows the transmission of broadband signals over long distances. Optical amplifiers compensate the power loss but they add noise. Moreover, a signal propagating in fiber experiences distortions due to chromatic dispersion and Kerr nonlinearity. The fiber channel thus suffers from three main impairments of different nature: noise, dispersion, and Kerr nonlinearity. The interaction between these three phenomena makes the problem of estimating the capacity challenging [1].

The work of H. Ghazlan was supported by a USC Annenberg Fellowship and the National Science Foundation (NSF) under Grant CCF-09-05235. The work of G. Kramer was supported by an Alexander von Humboldt Professorship endowed by the German Federal Ministry of Education and Research, as well as by the NSF under Grant CCF-09-05235. Part of the material in this paper was presented at the IEEE International Symposium on Information Theory, Austin, TX, June, 2010 and at the IEEE International Symposium on Information Theory, Saint Petersburg, Russia, July/August, 2011.

H. Ghazlan was with the Department of Electrical Engineering, University of Southern California, Los Angeles, CA 90089, USA. He is now with Intel Corporation, Hillsboro, OR 97124, USA. (e-mail: hassan.ghozlan@intel.com).

G. Kramer is with the Institute for Communications Engineering, Technical University of Munich, 80333 Munich, Germany (email: gerhard.kramer@tum.de).

A. Capacity Estimates

There are many approaches to estimate the capacity of optical fiber channels. The technical papers fall into two main categories: they either study the capacity of simplified models, or they develop capacity lower bounds (achievable rates) on the full model by simulation. We next review these papers. Our document belongs to the former category.

Splett et al [2] study a single-channel system and derive an approximate formula for the power spectral density of the intrachannel four-wave mixing (FWM) at the center frequency assuming the input signal has uncorrelated spectral components. They derive an achievable information rate expression by treating FWM as additive Gaussian noise. The information rate has a peak at a finite input power. They modify the power spectral density expression of FWM to obtain a similar result for multi-channel systems where cross-phase modulation (XPM) is ignored. Narimanov and Mitra [3] study a single-channel transmission over a multi-span dispersive fiber link. They use a perturbation technique to approximate the solution to the nonlinear Schrödinger (NLS) equation assuming that the nonlinear term is small and they derive a capacity expression. Xiang and Zhang [4] extend some of the results of [3].

Mecozzi [5] models the propagation of a single signal in a dispersionless fiber link, in which the fiber loss is compensated by distributed amplification. Mecozzi derives an expression for the conditional distribution of the output field given the input field by computing all (conditional) moments. Turitsyn et al [6] also study single-channel transmission over zero-dispersion fiber links. They obtain the conditional distribution using techniques from quantum mechanics. For Gaussian inputs, a sampling receiver and direct-detection, a lower bound on capacity is derived that grows logarithmically with the signal-to-noise ratio (SNR) with a pre-log = 1/2. In [7]–[9], Yousefi and Kschischang derive the conditional probability using two different approaches: a sum-product approach and a Fokker-Planck differential equation approach. Wei and Plant [10] make useful comments on the results of [6], [11] and [12].

Djordjevic et al [13] study a single-channel system and estimate numerically the achievable information rate for independent uniformly distributed inputs when the intrachannel Kerr nonlinearity, chromatic dispersion and amplified spontaneous emission are taken into account. They use a finite-state machine approach where the state is determined by a number of past and future inputs surrounding the current input, and the conditional distribution of the output given the state is approximated using histograms. Ivakovic et al [14] follow [13] and propose an approximate expression for the conditional output distribution when on-off keying (OOK) is used to

circumvent the computation of histograms. These methods are limited to low-order modulation for complexity reasons.

Mitra and Stark [11] study a wavelength division multiplexing (WDM) system in which XPM is the only nonlinear effect, i.e., they ignore FWM and assume that self-phase modulation (SPM) can be fully corrected. A key simplification in [11] is approximating the sum of intensities of the interfering channels in the XPM term of the propagation equation by a Gaussian random process. A lower bound on capacity (per WDM channel) is derived for Gaussian inputs using the input-output covariance matrix. The conclusion of [11] is that the lower bound has a peak and does not increase indefinitely with the input power. Wegener et al [15] also study WDM transmission over a multi-span dispersive fiber link. To simplify the solution of the coupled propagation equations analytically, the technique of [11] is used and the FWM is replaced with a Gaussian random process. A lower bound on capacity is evaluated using the input-output covariance matrix.

Ho and Kahn [16] study WDM transmission over a multi-span dispersive fiber link. They argue that under constant-envelope (or constant-intensity) modulation with uniform phase¹, SPM and XPM cause only time-invariant phase shifts and hence the phase distortion is eliminated. By modeling FWM as additive Gaussian noise, they obtain an estimate of the information rate achieved by constant-envelope modulation. The FWM components from individual fiber spans are assumed to combine incoherently.

Tang [12] studies WDM transmission over a single-span dispersion-free fiber link. In this case, the propagation equation can be solved analytically in closed-form. A lower bound on capacity is obtained for Gaussian inputs by computing the power spectral density of the input (the sum over all WDM channels), the power spectral density of the output (the overall WDM signal after propagation) and the cross-spectral density of the input and output. Tang extends the results of [12] to a multi-span dispersion-free fiber link in [17] and then to a multi-span dispersive fiber link in [18]. In [18], a truncated Volterra series [19] is used to approximate the solution to the NLS equation assuming that the effect of nonlinearity is small. The lower bounds in [12], [17] and [18] have a peak value at finite input powers.

Taghavi et al [20] study WDM transmission over a single-span dispersive fiber link. They use a (truncated) Volterra series solution to the propagation equation. Each receiver uses a linear filter to compensate dispersion followed by a matched filter (matched to the transmitted pulse) whose output is sampled at the symbol rate. Assuming that dispersion is weak (so that inter-symbol interference can be neglected), a discrete-time memoryless model is obtained. Each receiver has access to the received signal of all channels and thus this case is treated as a multiple-access channel. It is found that nonlinearity does not affect the capacity to the first-order approximation (in the nonlinear coefficient) and high rates are achieved by performing interference cancellation before decoding. Moreover, single-channel detection (i.e., the decoder

for a given user has access to the received signal at its own wavelength only) is considered in two regimes: XPM-dominated and FWM-dominated regimes. The capacity for single-channel detection is significantly reduced compared to the multiple access channel capacity.

Essiambre et al [1] review fundamental concepts of digital communications, information theory and the physical phenomena present in transmission over optical fiber networks. They estimate by numerical simulations capacity lower bounds for WDM using multi-ring constellations, different constellation shapings and different fiber dispersion maps. Nonlinear compensation through backpropagation of individual channels is used. The trend in the various scenarios is that the capacity lower bound has a peak value at a finite launch power.

Bosco et al [21], [22] study WDM transmission over uncompensated optical fiber links with both distributed and lumped amplification. They argue that, after digital signal processing (DSP) at the receiver, the distribution of each of the received constellation points is approximately Gaussian with independent components, even in the absence of additive ASE noise. Hence, they adopt a model, called the Gaussian noise (GN) model, in which the impact of nonlinear propagation is approximated by excess additive Gaussian noise (see also [2]). Using the GN model, capacity estimates are derived. In [23], Poggiolini discusses the GN model in depth.

Mecozzi and Essiambre [24] study multi-channel transmission over a dispersive fiber link with distributed amplification. They develop a first-order perturbation theory of the signal propagation and simplify the expression for highly dispersive, or pseudolinear, transmission. The signal is linearly-modulated² at the transmitter and the detection apparatus at the receiver is made of an optical filter to separate the channel, mixing with a local oscillator and subsequent sampling at the symbol rate. By concentrating on inter-channel nonlinearity, in particular XPM, they derive a capacity estimate per channel. An important observation is that the kurtosis of the constellation of the interfering channels is important in determining the system impairments.

Secondini et al [25] study WDM transmission over a dispersive fiber link. FWM is neglected. The key simplification is replacing the unknown intensities appearing in the propagation equation with those corresponding to linear propagation. They then derive a first-order approximation to the solution based on frequency-resolved logarithmic perturbations. The approximate solution is used to develop a linear time-varying discrete-time model for the channel which is composed of the optical fiber link followed by a back-propagation block (and thus it is assumed that SPM is fully compensated), a matched filter, and sampling at the symbol rate. By using the theory of mismatched decoding, they compute the information rate achieved by independent and identically distributed (i.i.d.) Gaussian input symbols and a maximum likelihood *symbol-by-symbol* detector designed for a memoryless additive white Gaussian noise (AWGN) auxiliary channel with the same covariance matrix as the true channel. They also evaluate the information rate achieved by a maximum likelihood *sequence* decoder

¹We refer to constant-envelope modulation with uniform phase as *ring* modulation.

²The signal is the sum of modulated pulses.

designed for an auxiliary AWGN channel with inter-symbol interference, and with the same input-output covariance matrix as the true channel.

Dar et al [26] propose a block-memoryless discrete-time channel model for WDM transmission in the pseudo-linear regime in which XPM is the dominant nonlinear effect. The model is a discrete-time phase noise channel in which the phase noise process models XPM and is assumed to be a block-independent process, i.e., it remains unchanged within a block but changes independently between blocks. It is assumed that the phase noise is (real) Gaussian with zero mean and a variance that depends on the type of modulation. For the proposed model, two lower bounds on capacity are developed: the first is tight in the low power regime while the second is better at high power. In [27], [28], Dar et al add an extra term to capture nonlinear effects that do not manifest themselves as phase noise. Agrell et al [29] propose a discrete-time model called the *finite-memory GN model* for coherent long-haul fiber links without dispersion compensation. Using the finite-memory GN model, they derive semi-analytic lower bounds for non i.i.d. inputs. Numerical simulations show that the information rates of the finite-memory GN model are higher than the rates of the regular GN model. We remark that the proposed discrete-time model is not derived from a continuous-time description of the system.

Yousefi and Kschischang [30]–[34] discuss the nonlinear Fourier transform (NFT), a method for solving a broad class of nonlinear differential equations, and in particular for solving the NLS equation for noiseless propagation. They propose a scheme, called nonlinear frequency-division multiplexing (NFDm), which can be viewed as a nonlinear analogue of orthogonal frequency-division multiplexing (OFDM). In NFDm, information is encoded in the NFT of the signal consisting of two components: a discrete and a continuous spectral function. By modulating non-interacting degrees of freedom of a signal, deterministic crosstalk between signal components due to dispersion and nonlinearity is eliminated, i.e., inter-symbol and inter-channel interference are zero if there is no noise.

B. Contributions and Organization

We develop discrete-time interference channel models for WDM transmission over a single span of both dispersionless and dispersive fiber. The models are based on coupled differential equations that capture SPM, XPM and group velocity mismatch (GVM). Transmitters send linearly-modulated pulses while receivers use matched filters with symbol rate sampling (for dispersionless transmission) or banks of filters (for dispersive transmission). Rather than using Gaussian codebooks, we design codebooks based on a new technique called *interference focusing*. We show that all users achieve a pre-log of 1 simultaneously by using interference focusing. This paper extends the results in [35] and [36]. More specifically, we extend the two-user model with a rectangular pulse in the non-zero GVM case to a three-user model with a general time-limited (of one symbol interval) pulse and we also derive a capacity outer bound. We highlight two aspects of our work (including [35] and [36]):

- We study an *interference channel* model for multiuser communication in nonlinear optical fiber. In contrast, most models in the literature reduce interference to be an additional source of noise and treat the problem as a *point-to-point channel*.
- We derive precise discrete-time models from continuous-time models with noise and filtering. In contrast, many publications derive or assume simplified discrete-time models based on direct sampling of the continuous-time received signals without filtering.

The paper is organized as follows. In Sec. II, we describe the wave propagation equation in optical fiber and the impairments that arise in transmission. We study the case of zero group velocity mismatch (zero dispersion) in Sec. III. We extend this model to non-zero group velocity mismatch in Sec. IV. For both cases, we develop discrete-time interference channel models and show that a pre-log of 1 is achievable for all users, despite XPM that arises due to the fiber nonlinearity. Sec. V relates interference focusing to interference alignment. Sec. VI concludes the paper.

C. Notation

We use common notation for probability distributions and information-theoretic quantities. Random variables are usually written as uppercase letters and their realizations as lowercase letters. Probability distributions and densities are labeled with the random variables, e.g., the probability density of X is written as $p_X(\cdot)$ and the conditional probability density of Y given X evaluated at $Y = y$ and $X = x$ is written as $p_{Y|X}(y|x)$. The expectation of X is denoted by $\mathbb{E}[X]$. The expressions $H(X)$, $H(Y|X)$, $H(XY)$ represent the entropy of X , the conditional entropy of Y given X , and the joint entropy of XY . The expressions $h(X)$, $h(Y|X)$, $h(XY)$ represent differential entropies. The mutual information of X and Y is written as $I(X;Y)$, and the mutual information of X and Y conditioned on Z is written as $I(X;Y|Z)$.

II. FIBER MODELS

We next discuss noise, chromatic dispersion and Kerr nonlinearity in optical fiber. Amplifiers add noise to the signal due to amplified spontaneous emission (ASE). The noise is typically modeled as a white Gaussian process. There are two types of amplification: lumped and distributed. In lumped amplification, N_s amplifiers are inserted periodically over a fiber link of total length L which creates N_s spans, often each of the same length $L_s = L/N_s$. A commonly-used lumped amplifier is the erbium-doped optical amplifier (EDFA). In distributed amplification, the signal is amplified continuously as it propagates through the fiber. Distributed amplification is accomplished by using Raman pumping. For multispan lumped or distributed amplification, signal-noise interaction occurs because of fiber nonlinearity. However, there is no signal-noise interaction in the single-span lumped amplification case, and this is the case we consider for the rest of the paper for simplicity. This model is sometimes used as an approximation when the noise is weak and the launch power is low.

Dispersion arises because the medium absorbs energy through the oscillations of bound electrons, causing a *frequency* dependence of the material refractive index [37, p. 7]. The Kerr effect is caused by anharmonic motion of bound electrons in the presence of an intense electromagnetic field, causing an *intensity* dependence of the material refractive index [37, p. 17, 165].

Suppose an optical field propagates at a center/carrier frequency ω_0 . Let $A(z, t)$ be a complex number representing the slowly-varying component (or envelope) of a linearly-polarized, electric field at position z and time t in single-mode fiber. We ignore polarization effects, i.e., a linearly-polarized input electric field remains linearly polarized during propagation. The equation governing the evolution of $A(z, t)$ as the wave propagates through the fiber is [37, p. 44]

$$\frac{\partial A}{\partial z} + \beta_1 \frac{\partial A}{\partial t} + i \frac{\beta_2}{2} \frac{\partial^2 A}{\partial t^2} = i \gamma |A|^2 A \quad (1)$$

where $i = \sqrt{-1}$, β_1 is the reciprocal of the group velocity, β_2 is the group velocity dispersion (GVD) coefficient, and γ is the nonlinear coefficient. It is common to specify GVD through the dispersion parameter D which is related to β_2 by [37, p. 11]

$$D = -\frac{2\pi c \beta_2}{\lambda_0^2} \quad (2)$$

where λ_0 is the wavelength in free-space, i.e., $\lambda_0 = 2\pi c/\omega_0$, and c is the speed of light in free space. By defining a retarded-time reference frame with $T = t - \beta_1 z$, we have

$$i \frac{\partial A}{\partial z} - \frac{\beta_2}{2} \frac{\partial^2 A}{\partial T^2} + \gamma |A|^2 A = 0 \quad (3)$$

which is referred to as the nonlinear Schrödinger (NLS) equation because of its similarity to the Schrödinger equation with a nonlinear potential term when the roles of time and distance are exchanged [37, p. 50]. The NLS equation has no closed-form solution for general inputs. Closed-form solutions to the NLS equation exist when $\beta_2 = 0$ and/or $\gamma = 0$. Solutions to the NLS equation with $\beta_2 \neq 0$ and $\gamma \neq 0$ exist only for special input waves called solitons.

There are other interesting cases where closed-form solutions exist. Consider a three-channel WDM system in which three optical fields at different center frequencies ω_1 , ω_2 and ω_3 are launched into the fiber, i.e., the input field is³

$$A(0, t) = \sum_{k=1}^3 A_k(0, t) e^{-i(\omega_k - \omega_0)t}. \quad (4)$$

Suppose $A(z, t)$ takes the form

$$A(z, t) = \sum_{k=1}^3 A_k(z, t) e^{i\hat{\beta}(\omega_k)z} e^{-i(\omega_k - \omega_0)t} \quad (5)$$

³ We ignore the frequency dependence of the modal distribution. The difference is small and can be neglected in practice [37, 7.1.2].

where $\hat{\beta}(\omega) = \beta_1(\omega - \omega_0) + (\beta_2/2)(\omega - \omega_0)^2$. By substituting into (1), we have⁴

$$\sum_{k=1}^3 e^{i\hat{\beta}(\omega_k)z} e^{-i(\omega_k - \omega_0)t} \left[i \frac{\partial A_k}{\partial z} + i \beta_{1k} \frac{\partial A_k}{\partial t} - \frac{\beta_{2k}}{2} \frac{\partial^2 A_k}{\partial t^2} + \gamma_k (|A_k|^2 + 2 \sum_{k' \neq k} |A_{k'}|^2) A_k \right] + F = 0 \quad (6)$$

where $\beta_{1k} = \beta_1 + \beta_2(\omega_k - \omega_0)$, $\beta_{2k} = \beta_2$, $\gamma_k = \gamma$ and

$$F = \sum_{k_1 \neq k_2, k_3 \neq k_2} e^{i\hat{\beta}(\omega_{k_1} - \omega_{k_2} + \omega_{k_3})z} e^{-i(\omega_{k_1} - \omega_{k_2} + \omega_{k_3} - \omega_0)t} \times \left[A_{k_1} A_{k_2}^* A_{k_3} e^{i\Delta\hat{\beta}(\omega_{k_1}, \omega_{k_2}, \omega_{k_3})z} \right] \quad (7)$$

with $\Delta\hat{\beta}(\omega_{k_1}, \omega_{k_2}, \omega_{k_3})$ defined as

$$\Delta\hat{\beta} = \hat{\beta}(\omega_{k_1}) - \hat{\beta}(\omega_{k_2}) + \hat{\beta}(\omega_{k_3}) - \hat{\beta}(\omega_{k_1} - \omega_{k_2} + \omega_{k_3}).$$

The summands in (7) are called FWM terms because they involve mixing, i.e., energy transfer, between four frequencies: ω_{k_1} , ω_{k_2} , ω_{k_3} and $\omega_{k_1} - \omega_{k_2} + \omega_{k_3}$ for $k_1 \neq k_2$, $k_3 \neq k_2$. We remark that the phase-matching condition $\Delta\hat{\beta} = 0$ should be satisfied for new frequency components to build up significantly via FWM, a condition not generally satisfied in practice when there is dispersion [37, Sec. 7.1.1].

We ignore all FWM terms, i.e., we set $F = 0$ in (6). Therefore, we have the coupled equations

$$i \frac{\partial A_k}{\partial z} + i \beta_{1k} \frac{\partial A_k}{\partial t} - \frac{\beta_{2k}}{2} \frac{\partial^2 A_k}{\partial t^2} + \gamma_k (|A_k|^2 + 2 \sum_{k' \neq k} |A_{k'}|^2) A_k = 0 \quad (8)$$

for $k = 1, 2, 3$, assuming that the three optical fields do not overlap in the frequency domain. There are two nonlinear terms in (8): the first is referred to as SPM and the second term is referred to as XPM. The term *phase modulation* is because, in absence of GVD, Kerr nonlinearity leaves the pulse shape unchanged but causes an intensity-dependent phase shift due to the signal *itself* (SPM) and *co-propagating* signals (XPM). XPM is an important impairment in optical networks using WDM, see [1]. There are also two terms in (8) due to dispersion. The first term with β_{1k} captures the mismatch in group velocity *between* channels while the second term with β_{2k} captures the GVD *within* the bandwidth of a channel.

Similar to the NLS equation (3), the coupled equations in (8) have no closed-form solution for a general input. Therefore, we make a further simplification by ignoring the GVD within a channel, i.e., we set $\beta_{2k} = 0$ for $k = 1, 2, 3$. This simplification gives the closed-form solution:⁵

$$A_k(L, t) = A_k(0, t - \beta_{k1}L) \exp(i\phi_k(L, t - \beta_{k1}L)) \quad (9)$$

⁴ We do not use a retarded frame because it does not lead to much simplification. This is because it is not possible to eliminate simultaneously all the terms of first-order derivatives with respect to time.

⁵ The solution follows from steps similar to the steps outlined in Sec. 1.8.10 of [38] for two coupled equations.

GVM	Pulse	Users	Sec.
No	rectangular	two	III-A
No	rectangular	three	III-E
Yes	general time-limited	three	IV-B

TABLE I
ASSUMPTIONS FOR DISCRETE-TIME MODELS

where $k \in \{1, 2, 3\}$, L is the length of a single span of fiber and the time-dependent nonlinear phase shifts $\phi_k(L, t)$ are

$$\phi_1(L, t) = \int_0^L \gamma_1 (|A_1(0, t)|^2 + 2|A_2(0, t + d_{12}\zeta)|^2 + 2|A_3(0, t + d_{13}\zeta)|^2) d\zeta \quad (10)$$

$$\phi_2(L, t) = \int_0^L \gamma_2 (|A_2(0, t)|^2 + 2|A_1(0, t + d_{21}\zeta)|^2 + 2|A_3(0, t + d_{23}\zeta)|^2) d\zeta \quad (11)$$

$$\phi_3(L, t) = \int_0^L \gamma_3 (|A_3(0, t)|^2 + 2|A_1(0, t + d_{31}\zeta)|^2 + 2|A_2(0, t + d_{32}\zeta)|^2) d\zeta \quad (12)$$

where

$$d_{kj} \triangleq \beta_{1k} - \beta_{1j} \quad (13)$$

is a measure of GVM between channel k and channel j . We remark that our model captures GVD of the *overall* signal, but only through GVM, namely through $d_{kj} = \beta_2(\omega_k - \omega_j)$.

As we pointed out earlier, we assume lumped amplification at the receiver, i.e., the signal observed at receiver k after removing the constant phase shift $e^{i\hat{\beta}(\omega_k)L}$ is

$$r_k(t) = A_k(L, t) + z_k(t) \quad (14)$$

where $z_k(t)$ is circularly-symmetric white Gaussian noise with $\mathbb{E}[z_k(t)] = 0$, and $\mathbb{E}[z_k(t)z_k^*(t + \tau)] = N\delta(\tau)$. The processes $z_1(t)$, $z_2(t)$ and $z_3(t)$ are statistically independent.

Suppose the transmitted signals are linearly-modulated, i.e., the signal sent by transmitter k is

$$A_k(0, t) = \sum_{m=0}^{n-1} x_k[m] p(t - mT_s) \quad (15)$$

where $(x_k[0], \dots, x_k[n-1])$ is the codeword of transmitter k and $p(t)$ is a pulse such that $p(t) = 0$ for $t \notin [0, T_s]$ and

$$\int_0^{T_s} |p(\lambda)|^2 d\lambda = E_s. \quad (16)$$

We analyze the setup above in two steps.

- 1) We start with a simplified version in Sec. III where GVM is neglected, i.e., β_{1k} is taken to be the same for all k so that $d_{kj} = 0$ for all k, j . For simplicity, we use a rectangular pulse $p(t)$ and consider mainly two WDM channels.
- 2) We use the insights gained from Sec. III to address the three-user model with GVM and general (time-limited) pulses in Sec. IV.

Table I summarizes the assumptions.

III. ZERO GROUP VELOCITY MISMATCH

Consider zero GVM with a rectangular pulse (in the time domain) and $E_s = 1$. We present a discrete-time two-user channel model in Sec. III-A, and we show that a pre-log 1/2 is achievable for two users by using either pure amplitude modulation (Sec. III-B) or pure phase modulation (Sec. III-C). We introduce interference focusing in Sec. III-D and show that it achieves a pre-log 1 for both users, and therefore no degrees of freedom are lost. An extension of the discrete-time model to three users is presented in Sec. III-E.

A. Discrete-Time Two-User Model

Consider a two-user system in which receiver k , $k = 1, 2$, obtains $(Y_k[0], Y_k[1], \dots, Y_k[n-1])$ by matched filtering the received signal $r_k(t)$ and sampling the filter output at the symbol rate. Equations (9–11) and (14), with $\beta_{11} = \beta_{12}$ and $A_3(0, t) = 0$, imply that the channel is memoryless. Hence, we drop the time indices and write the input-output relationships as

$$Y_1 = X_1 \exp(ih_{11}|X_1|^2 + ih_{12}|X_2|^2) + Z_1 \quad (17)$$

$$Y_2 = X_2 \exp(ih_{21}|X_1|^2 + ih_{22}|X_2|^2) + Z_2 \quad (18)$$

where Z_k is circularly-symmetric complex Gaussian noise with variance N . The noise random variables at the receivers are independent. The term $\exp(ih_{kk}|X_k|^2)$ models SPM and the term $\exp(ih_{k\ell}|X_\ell|^2)$, $k \neq \ell$, models XPM. We regard the $h_{k\ell}$ as *channel coefficients* that are time invariant. These coefficients are known at the transmitters as well as the receivers. We use symmetric power constraints

$$\mathbb{E}[|X_k|^2] \leq P, \quad k = 1, 2 \quad (19)$$

but the results below generalize to asymmetric powers.

A *scheme* is a collection $\{(\mathcal{C}_1(P, N), \mathcal{C}_2(P, N))\}$ of pairs of codes indexed by (P, N) , such that user k uses the code $\mathcal{C}_k(P, N)$ that satisfies the power constraint and achieves an information rate $R_k(P, N)$ where $k = 1, 2$. We distinguish between two limiting cases: 1) fixed noise with growing powers and 2) fixed powers with vanishing noise.

Definition 1: The *high-power* pre-log pair (\bar{r}_1, \bar{r}_2) is achieved by a scheme if the rates satisfy

$$\bar{r}_k(N) = \lim_{P \rightarrow \infty} \frac{R_k(P, N)}{\log(P/N)} \text{ for } k = 1, 2. \quad (20)$$

Definition 2: The *low-noise* pre-log pair (r_1, r_2) is achieved by a scheme if the rates satisfy

$$r_k(P) = \lim_{N \rightarrow 0} \frac{R_k(P, N)}{\log(P/N)} \text{ for } k = 1, 2. \quad (21)$$

The (high-power or low-noise) pre-log pair $(1/2, 1/2)$ can be achieved if both users use amplitude modulation only or phase modulation only, as shown in Sec. III-B and Sec. III-C, respectively. We show in Sec. III-D that the high-power pre-log pair $(1, 1)$ can be achieved through *interference focusing*.

B. Amplitude Modulation

First, we introduce a result by Lapidoth [39, Sec. IV].

Lemma 3: Let $Y = X + Z$ where Z is a circularly-symmetric complex Gaussian random variable with mean 0 and variance N . Define $S = |X|^2/P$. Suppose S is distributed as

$$p_S(s) = \frac{e^{-s/2}}{\sqrt{2\pi s}}, \quad s \geq 0. \quad (22)$$

In other words, $|X|^2$ follows a Gamma distribution (or a Chi-squared distribution) with *one* degree of freedom and has mean P . Then we have

$$I(|X|^2; |Y|^2) \geq \frac{1}{2} \log \left(\frac{P}{2N} \right) + o(1) \quad (23)$$

where $o(1)$ tends to zero as P/N tends to infinity. ■

If $|X_1|^2/P$ and $|X_2|^2/P$ are distributed according to p_S in (22), then we have for $k = 1, 2$

$$I(X_k; Y_k) \geq I(|X_k|; |Y_k|) = I(|X_k|^2; |Y_k|^2) \quad (24)$$

and it follows from (23) that

$$I(X_k; Y_k) \geq \frac{1}{2} \log \left(\frac{P}{2N} \right) + o(1). \quad (25)$$

It follows that the high-power and low-noise pre-log pair $(1/2, 1/2)$ can be achieved when both users use amplitude modulation.

C. Phase Modulation

Suppose the transmitters use phase modulation with $|X_1| = \sqrt{P}$ and $|X_2| = \sqrt{P}$. The input-output equations (17)–(18) become

$$Y_1 = X_1 e^{ih_{11}P + ih_{12}P} + Z_1 \quad (26)$$

$$Y_2 = X_2 e^{ih_{21}P + ih_{22}P} + Z_2. \quad (27)$$

Therefore, each receiver sees a constant phase shift which allows us to treat each transmitter-receiver pair separately as an AWGN channel. We next show that the pre-log pair $(r_1, r_2) = (1/2, 1/2)$ can be achieved by using phase modulation only.

Theorem 4 (One-Ring Modulation): Fix $P > 0$. Let $Y = X + Z$ where Z is a circularly-symmetric complex Gaussian random variable with mean 0 and variance N , and $X = \sqrt{P}e^{i\Phi_X}$ where Φ_X is a real random variable uniformly distributed on $[0, 2\pi)$. Then we have

$$I(X; Y) \geq \frac{1}{2} \log \left(\frac{2P}{N} \right) - 1 \text{ (nats)}. \quad (28)$$

Proof: We have

$$I(X; Y) = \mathbb{E}[-\log p_Y(Y)] - \log(\pi e N) \quad (29)$$

The pdf p_Y of Y can be shown to be [1, p. 688]

$$p_Y(y) = \frac{1}{\pi N} e^{-(y_A^2 + P)/N} I_0 \left(\frac{2y_A \sqrt{P}}{N} \right) \quad (30)$$

where $I_0(\cdot)$ is the modified Bessel function of the first kind of order zero and $y_A = |Y|$. Therefore, we have

$$\begin{aligned} h(Y) &= \mathbb{E} \left[-\log \left(\frac{1}{\pi N} e^{-(Y_A^2 + P)/N} I_0 \left(\frac{2Y_A \sqrt{P}}{N} \right) \right) \right] \\ &\stackrel{(a)}{\geq} \mathbb{E} \left[-\log \left(\frac{1}{\pi N} \frac{e^{-(Y_A - \sqrt{P})^2/N}}{\sqrt{2Y_A \sqrt{P}/N}} \right) \right] \\ &\stackrel{(b)}{\geq} \mathbb{E} \left[\log \left(\pi N \sqrt{2Y_A \sqrt{P}/N} \right) \right] \\ &= \frac{1}{4} \log \left(\frac{2P}{N} \right) + \log(\pi N) + \frac{1}{2} \mathbb{E} \left[\log \left(Y_A \sqrt{\frac{2}{N}} \right) \right] \end{aligned} \quad (31)$$

where (a) follows by using Lemma 9 in Appendix A and (b) holds because $(Y_A - \sqrt{P})^2 \geq 0$. The pdf of Y_A is given by

$$\begin{aligned} p_{Y_A}(y_A) &= \int_{-\pi}^{\pi} p_Y(y) y_A d\phi_y \\ &= \frac{2y_A}{N} e^{-(y_A^2 + P)/N} I_0 \left(\frac{2y_A \sqrt{P}}{N} \right). \end{aligned} \quad (32)$$

The last expectation in (31) is

$$\begin{aligned} \mathbb{E} \left[\log \left(Y_A \sqrt{\frac{2}{N}} \right) \right] &= \int_0^\infty p_{Y_A}(y_A) \log \left(y_A \sqrt{\frac{2}{N}} \right) dy_A \\ &\stackrel{(a)}{=} \int_0^\infty z e^{-(z^2 + \nu^2)/2} I_0(z\nu) \log(z) dz \\ &\stackrel{(b)}{=} \frac{1}{2} \left[\Gamma \left(0, \frac{P}{N} \right) + \log \left(\frac{2P}{N} \right) \right] \\ &\stackrel{(c)}{\geq} \frac{1}{2} \log \left(\frac{2P}{N} \right) \end{aligned} \quad (33)$$

where $\Gamma(a, x)$ is the upper incomplete Gamma function, see (133) below. Step (a) follows by setting $\nu^2 = 2P/N$ and $z = y_A \sqrt{2/N}$, (b) follows from Lemma 12 in Appendix B and (c) holds because $\Gamma(0, x) \geq 0$ for $x \geq 0$.⁶ Combining (29), (31) and (33) concludes the proof. ■

Now, suppose that $X_k = \sqrt{P}e^{i\Phi_{X,k}}$ for $k = 1, 2$ where $\Phi_{X,1}$ and $\Phi_{X,2}$ are statistically independent and uniformly distributed on $[0, 2\pi)$. It follows from (26), (27) and Theorem 4 that the high-power and low-noise pre-log pair $(1/2, 1/2)$ can be achieved when both users use phase modulation.

D. Interference Focusing

We propose an *interference focusing* technique in which the transmitters *focus* their phase interference on one point by constraining their transmitted signals to satisfy

$$h_{21}|X_1|^2 = 2\pi\tilde{n}_1, \quad \tilde{n}_1 = 1, 2, 3, \dots \quad (34)$$

$$h_{12}|X_2|^2 = 2\pi\tilde{n}_2, \quad \tilde{n}_2 = 1, 2, 3, \dots \quad (35)$$

In other words, the transmitters use *multi-ring modulation* with specified spacings between the rings.⁷ We thereby remove

⁶Note that $\lim_{x \rightarrow \infty} \Gamma(0, x) = 0$.

⁷Multi-ring modulation was used in [1], [40], [41] for symmetry and computational reasons. We here find that it is useful for improving rate.

XPM interference and (17)-(18) reduce to

$$Y_k = X_k e^{i h_{kk} |X_k|^2} + Z_k, \quad k = 1, 2. \quad (36)$$

This channel is effectively an AWGN channel since h_{kk} is known by receiver k and the SPM phase shift is determined by the desired signal X_k . We will show that the high-power pre-log pair (1, 1) is achieved under the constraints (34)-(35).

Theorem 5 (Multi-Ring Modulation): Let $Y = X + Z$ where Z is a circularly-symmetric complex Gaussian random variable with mean 0 and variance N . Suppose $\mathbb{E}[|X|^2] \leq P$ and $|X|^2$ is allowed to take on values that are multiples of a fixed real number $\hat{p} > 0$, i.e., $|X|^2 = m\hat{p}$ where $m \in \mathbb{N}$. Then there exists a probability distribution p_X of X such that

$$\lim_{P \rightarrow \infty} \frac{I(X; Y)}{\log(P/N)} \geq 1. \quad (37)$$

Proof: Define $X_A = |X|$ and $\Phi_X = \arg X$. Consider multi-ring modulation, i.e., X_A and Φ_X are statistically independent, Φ_X is uniformly distributed on the interval $[0, 2\pi)$ and $X_A \in \{\sqrt{P_j} : j = 1, \dots, J\}$ where J is the number of rings. We choose the rings to be spaced uniformly in amplitude as

$$P_j = a j^2 \hat{p} \quad (38)$$

where a is a positive integer. We further use a uniform frequency of occupation of rings with $P_{X_A}(\sqrt{P_j}) = 1/J$, $j = 1, 2, \dots, J$. The power constraint is therefore

$$\frac{1}{J} \sum_{j=1}^J a j^2 \hat{p} \leq P. \quad (39)$$

For (39), we compute

$$\frac{1}{J} \sum_{j=1}^J a \hat{p} j^2 = a \hat{p} \frac{(J+1)(2J+1)}{6} \quad (40)$$

and to satisfy the power constraint we choose⁸

$$J = \frac{-3 + \sqrt{1 + 48P/(a\hat{p})}}{4}. \quad (41)$$

Moreover, we choose $a = \lfloor \max\{1, N \log(P/N)\} \rfloor$. We remark that we say $f(x)$ scales as $g(x)$ if

$$\lim_{x \rightarrow \infty} \frac{f(x)}{g(x)} = \text{constant}.$$

For example, J scales as $\sqrt{(P/N)/\log(P/N)}$ when a is chosen as above, i.e., we have

$$\lim_{P \rightarrow \infty} \frac{J}{\sqrt{(P/N)/\log(P/N)}} = \text{constant}.$$

We have

$$\begin{aligned} I(X; Y) &= I(X_A \Phi_X; Y) \\ &= I(X_A; Y) + I(\Phi_X; Y | X_A) \end{aligned} \quad (42)$$

The term $I(X_A; Y)$ can be viewed as the amplitude contribution while the term $I(\Phi_X; Y | X_A)$ is the phase contribution.

⁸The solution for J should be positive and rounded down to the nearest integer but we ignore these issues for notational simplicity.

1) Phase Contribution: We show that the phase modulation contributes at least 1/2 to the pre-log when using multi-ring modulation.

Lemma 6: For integers a and b with $a \leq b$, a non-decreasing function $f(x)$ in x satisfies

$$\int_{a-1}^b f(x) dx \leq \sum_{i=a}^b f(i). \quad (43)$$

We thus have

$$\begin{aligned} I(\Phi_X; Y | X_A) &\stackrel{(a)}{=} \sum_{j=1}^J \frac{1}{J} I(\Phi_X; Y | X_A = \sqrt{P_j}) \\ &\stackrel{(b)}{\geq} \sum_{j=1}^J \frac{1}{J} \frac{1}{2} \log \left(\frac{P_j}{N} \right) - 1 \\ &\stackrel{(c)}{=} \frac{1}{2J} \sum_{j=1}^J \log \left(\frac{a j^2 \hat{p}}{N} \right) - 1 \\ &\stackrel{(d)}{\geq} \frac{1}{2J} \int_0^J \log \left(\frac{a x^2 \hat{p}}{N} \right) dx - 1 \\ &\stackrel{(e)}{=} \frac{1}{2} \log \left(\frac{a J^2 \hat{p}}{N e^2} \right) - 1 \end{aligned} \quad (44)$$

where (a) follows from the uniform occupation of rings, (b) follows from Theorem 4, (c) holds by choosing the rings according to (38), (d) follows from Lemma 6 since the logarithm is an increasing function and (e) follows by using $\log(ax^2 \hat{p}/N) = \log(a \hat{p}/N) + 2 \log(x)$ and

$$\int \log(x) dx = x \log(x/e). \quad (45)$$

We can therefore write

$$\lim_{P \rightarrow \infty} \frac{I(\Phi_X; Y | X_A)}{\log(P/N)} \geq \lim_{P \rightarrow \infty} \frac{\frac{1}{2} \log(a J^2 \hat{p}/N)}{\log(P/N)} = \frac{1}{2} \quad (46)$$

where (46) follows because a scales as $N \log(P/N)$, J^2 scales as $(P/N)/\log(P/N)$, and \hat{p} is independent of P and N . The pre-log of the phase contribution is therefore at least 1/2.

2) Amplitude Contribution: We show that amplitude modulation contributes 1/2 to the pre-log. We have

$$I(X_A; Y) = H(X_A) - H(X_A | Y) \quad (47)$$

where $H(X_A) = \log(J)$. We showed previously that J scales as $\sqrt{(P/N)/\log(P/N)}$ if a scales as $N \log(P/N)$. We bound $H(X_A | Y)$ using Fano's inequality as

$$\begin{aligned} H(X_A | Y) &\leq H(X_A | \hat{X}_A) \\ &\leq H(P_e) + P_e \log(J-1) \end{aligned} \quad (48)$$

where \hat{X}_A is any estimate of X_A given Y , $P_e = \Pr[\hat{X}_A \neq X_A]$ and $H(P_e)$ is the binary entropy function with a general logarithm base. Suppose we use the minimum distance estimator

$$\hat{X}_A = \arg \min_{x_A \in \mathcal{X}_A} |Y_A - x_A| \quad (49)$$

where $Y_A = |Y|$ and $\mathcal{X}_A = \{\sqrt{P_j} : j = 1, \dots, J\}$. The probability of error P_e is upper bounded by (see Lemma 13 in Appendix C)

$$P_e \leq \frac{2}{J} \sum_{j=2}^J \exp\left(-\frac{\Delta_j^2}{4}\right) \quad (50)$$

where $\Delta_j = (\sqrt{P_j} - \sqrt{P_{j-1}})/\sqrt{N}$. For the power levels (38), we have $\Delta_j = \sqrt{a\hat{p}/N}$ for all j , and hence

$$P_e \leq \frac{2(J-1)}{J} \exp\left(-\frac{a\hat{p}}{4N}\right) \leq 2 \exp\left(-\frac{a\hat{p}}{4N}\right). \quad (51)$$

We see from (51) that $\lim_{P \rightarrow \infty} P_e = 0$ if a scales as $N \log(P/N)$ (recall that J scales as $\sqrt{(P/N)/\log(P/N)}$). We thus have $\lim_{P \rightarrow \infty} H(X_A|Y) = 0$ by using (48). Consequently, we have

$$\lim_{P \rightarrow \infty} \frac{I(X_A; Y)}{\log(P/N)} = \lim_{P \rightarrow \infty} \frac{\log(J)}{\log(P/N)} = \frac{1}{2}. \quad (52)$$

Finally, combining (42), (46), and (52) gives (37). ■

We conclude that interference focusing achieves the largest-possible high-power pre-log of 1. Each user can therefore exploit all the phase and amplitude degrees of freedom simultaneously.

E. Discrete-Time Three-User Model

Consider a WDM system with three users. Receiver k obtains $(Y_k[0], Y_k[1], \dots, Y_k[n-1])$ by matched filtering the received signal $r_k(t)$ in (14) and sampling the filter output at the symbol rate. By setting $\beta_{11} = \beta_{12} = \beta_{13}$ in (9–12), we have the following memoryless channel model:

$$Y_k = X_k \exp\left(i \sum_{\ell=1}^3 h_{k\ell} |X_\ell|^2\right) + Z_k \quad (53)$$

for $k = 1, 2, 3$ where Z_k is circularly-symmetric complex Gaussian noise with variance N . All noise random variables at different receivers are statistically independent. The terms $\exp(ih_{kk}|X_k[j]|^2)$ model SPM and the terms $\exp(ih_{k\ell}|X_\ell[j]|^2)$, $\ell \neq k$, model XPM. The $h_{k\ell}$ are again *channel coefficients* that are time invariant and are known at the transmitters as well as the receivers. The power constraints are

$$\mathbb{E}[|X_k|^2] \leq P, \quad k = 1, 2, 3. \quad (54)$$

Interference Focusing: We outline how to apply interference focusing to the three-user channel. Define the interference phase vector

$$\underline{\Psi} \triangleq [\Psi_1, \Psi_2, \Psi_3]^T \quad (55)$$

where $\Psi_k = \sum_{\ell=1}^3 h_{k\ell} |X_\ell|^2$ and the instantaneous power vector

$$\underline{\Pi} \triangleq [|X_1|^2, |X_2|^2, |X_3|^2]^T. \quad (56)$$

The relationship between the $\underline{\Psi}$ and $\underline{\Pi}$ in matrix form is

$$\underline{\Psi} = H_{SP} \underline{\Pi} + H_{XP} \underline{\Pi} \quad (57)$$

where H_{SP} is a diagonal matrix that accounts for SPM and H_{XP} is a zero-diagonal matrix that accounts for XPM. For example, suppose the XPM matrix for a 3-user interference network is

$$H_{XP} = \begin{bmatrix} 0 & 1/2 & 3/5 \\ 3/4 & 0 & 2/3 \\ 5/6 & 1/5 & 0 \end{bmatrix}. \quad (58)$$

Suppose that each transmitter knows the channel coefficients between itself and all the receiving nodes. The transmitters can thus use power levels of the form

$$\begin{aligned} \underline{\Pi} &= 2\pi \cdot [\text{lcm}(4, 6)m_1, \text{lcm}(2, 5)m_2, \text{lcm}(5, 3)m_3] \\ &= 2\pi \cdot [12m_1, 10m_2, 15m_3] \end{aligned} \quad (59)$$

where $\text{lcm}(a, b)$ is the least common multiple of a and b , and m_1, m_2, m_3 are positive integers. We thus have

$$H_{XP} \underline{\Pi} = 2\pi \begin{bmatrix} 0 & 5 & 9 \\ 9 & 0 & 10 \\ 10 & 2 & 0 \end{bmatrix} \begin{bmatrix} m_1 \\ m_2 \\ m_3 \end{bmatrix} \quad (60)$$

which implies that the phase interference has been eliminated.

The above example combined with an analysis similar to Section III-D shows that interference focusing will give each user a pre-log of 1 even for three-user interference networks. However, the XPM coefficients $h_{k\ell}$ must be *rational*. This result can be generalized to the K -user case. Modifying interference focusing for *real-valued* XPM coefficients is an interesting problem. It is clear from the example that interference focusing does not require global channel state information.

IV. NON-ZERO GROUP VELOCITY MISMATCH

We next consider non-zero GVM, i.e., $\beta_{13} \neq \beta_{12} \neq \beta_{11}$. Without loss of generality, suppose that $\beta_{13} > \beta_{12} > \beta_{11}$. We now use a general time-limited pulse $p(t)$.

We start with the continuous-time model in Sec. IV-A below and derive a discrete-time model in Sec. IV-B. We show that a pre-log 1/2 is achievable for all users by using pure amplitude modulation in Sec. IV-C. Next, we show that interference focusing achieves a pre-log of at least 1 for all users under certain conditions in Sec. IV-D. Finally, we show in Sec. IV-E that interference focusing achieves the maximum pre-log of 1 and, therefore, interference focusing is pre-log optimal.

A. Continuous-Time Model

The signal $r_k(t)$ in (14) is fed to a bank of linear time-invariant (LTI) filters with impulse responses $\{h_f(t)\}_{f \in \mathcal{F}_k}$, where $\mathcal{F}_k \subset \mathbb{Z} = \{\dots, -1, 0, 1, \dots\}$ and

$$h_f(t) = p^*(-t) \exp(-i2\pi f K(-t)) \quad (61)$$

where $K(t)$ is defined as

$$K(t) = \frac{1}{E_s} \int_0^t |p(\lambda)|^2 d\lambda. \quad (62)$$

The choice of the set \mathcal{F}_k is specified in Sec. IV-D. We show in Appendix D that the impulse responses of the filters are orthogonal, i.e., if $f_1 \neq f_2$, then we have

$$\int_{-\infty}^{\infty} h_{f_1}(\xi) h_{f_2}^*(\xi) d\xi = 0. \quad (63)$$

The remaining analysis is similar for all receivers, hence we present the analysis for receiver 1 only. The output of the filter with index f is

$$y_{1,f}(t) = r_1(t) \star h_f(t) \quad (64)$$

where \star denotes convolution. The noiseless part $\tilde{y}_{1,f}(t)$ of the output of this filter is

$$\begin{aligned} \tilde{y}_{1,f}(t + \beta_{11}L) &\triangleq A_1(L, t + \beta_{11}L) \star h_f(t) \\ &= \left(A_1(0, t) e^{i\phi_1(L, t)} \right) \star h_f(t) \\ &= \left(\sum_{m=0}^{n-1} x_1[m] p(t - mT_s) e^{i\phi_1(L, t)} \right) \star h_f(t) \\ &= \sum_{m=0}^{n-1} x_1[m] \int p(\tau - mT_s) p^*(\tau - t) e^{i\phi_1(L, \tau) - i2\pi f K(\tau - t)} d\tau \end{aligned} \quad (65)$$

where the integral is over the whole real line. Sampling the output signal $y_{1,f}(t + \beta_{11}L)$ at the time instants $t = jT_s$, for $j = 1, 2, \dots, n$, yields

$$\begin{aligned} \tilde{y}_{1,f}(jT_s + \beta_{11}L) &= x_1[j] \int_{jT_s}^{jT_s + T_s} |p(\tau - jT_s)|^2 e^{i\phi_1(L, \tau) - i2\pi f K(\tau - jT_s)} d\tau \end{aligned} \quad (66)$$

where we used $p(t) = 0$ for $t \notin [0, T_s]$. We write $\phi_1(L, \tau)$ as

$$\phi_1(L, \tau) = \phi_{11}(L, \tau) + \phi_{12}(L, \tau) + \phi_{13}(L, \tau) \quad (67)$$

where we have defined

$$\phi_{11}(L, t) \triangleq \gamma_1 L |A_1(0, t)|^2 \quad (68)$$

$$\phi_{12}(L, t) \triangleq 2\gamma_1 L_{12} \frac{1}{T_s} \int_{t-Ld_{21}}^t |A_2(0, \lambda)|^2 d\lambda \quad (69)$$

$$\phi_{13}(L, t) \triangleq 2\gamma_1 L_{13} \frac{1}{T_s} \int_{t-Ld_{31}}^t |A_3(0, \lambda)|^2 d\lambda \quad (70)$$

and where $L_{1k} \triangleq T_s/|d_{1k}|$ for $k \neq 1$. Since $p(t) = 0$ for $t \notin [0, T_s]$, we have

$$\begin{aligned} \phi_{12}(L, t) &= \frac{2\gamma_1 L_{12}}{T_s} \int_{t-Ld_{21}}^t \sum_{m=0}^{n-1} |x_2[m]|^2 |p(\lambda - mT_s)|^2 d\lambda \\ &= \frac{2\gamma_1 L_{12}}{T_s} \sum_{m=0}^{n-1} |x_2[m]|^2 \int_{t-Ld_{21}}^t |p(\lambda - mT_s)|^2 d\lambda \\ &= 2\gamma_1 L_{12} \frac{E_s}{T_s} \sum_{m=0}^{n-1} |x_2[m]|^2 \psi(t - mT_s; d_{21}) \end{aligned} \quad (71)$$

where $\psi(t; d)$ is defined as

$$\psi(t; d) \triangleq \frac{1}{E_s} \int_{t-Ld}^t |p(\lambda)|^2 d\lambda. \quad (72)$$

If $Ld \geq T_s$, then

$$\psi(t; d) = \begin{cases} K(t), & 0 \leq t < T_s \\ 1, & T_s \leq t < Ld \\ \tilde{K}(t; d), & Ld \leq t < Ld + T_s \\ 0, & \text{otherwise} \end{cases} \quad (73)$$

where $K(t)$ is defined by (62) and $\tilde{K}(t; d)$ is given by

$$\begin{aligned} \tilde{K}(t; d) &= \frac{1}{E_s} \int_{t-Ld}^{T_s} |p(\lambda)|^2 d\lambda \\ &= \frac{1}{E_s} \int_0^{T_s} |p(\lambda)|^2 d\lambda - \frac{1}{E_s} \int_0^{t-Ld} |p(\lambda)|^2 d\lambda \\ &= 1 - K(t - Ld). \end{aligned} \quad (74)$$

One can express $\phi_{13}(L, t)$ in a similar manner. Suppose that $L|d_{1k}| = M_{1k}T_s$ for some positive integer M_{1k} for $k = 2, 3$. Hence, for $\tau \in [jT_s, jT_s + T_s]$, we have⁹

$$\phi_{11}(L, \tau) = \gamma_1 L \frac{E_s}{T_s} |x_1[j]|^2 \quad (75)$$

$$\begin{aligned} \phi_{12}(L, \tau) &= 2\gamma_1 L_{12} \frac{E_s}{T_s} \left(\left(\sum_{r=1}^{M_{12}} |x_2[j - r]|^2 \right) + \right. \\ &\quad \left. (|x_2[j]|^2 - |x_2[j - M_{12}]|^2) K(t - jT_s) \right) \end{aligned} \quad (76)$$

$$\begin{aligned} \phi_{13}(L, \tau) &= 2\gamma_1 L_{13} \frac{E_s}{T_s} \left(\left(\sum_{r=1}^{M_{13}} |x_3[j - r]|^2 \right) + \right. \\ &\quad \left. (|x_3[j]|^2 - |x_3[j - M_{13}]|^2) K(t - jT_s) \right). \end{aligned} \quad (77)$$

By substituting (75)–(77) in (67), we get

$$\phi_1(L, \tau) = \phi_1[j] + 2\pi v_1[j] K(\tau - jT_s) \quad (78)$$

where

$$\begin{aligned} \phi_1[j] &= h_{11} |x_1[j]|^2 + h_{12} \sum_{r=1}^{M_{12}} |x_2[j - r]|^2 \\ &\quad + h_{13} \sum_{r=1}^{M_{13}} |x_3[j - r]|^2 \end{aligned} \quad (79)$$

$$\begin{aligned} v_1[j] &= h_{12} (|x_2[j]|^2 - |x_2[j - M_{12}]|^2) / 2\pi \\ &\quad + h_{13} (|x_3[j]|^2 - |x_3[j - M_{13}]|^2) / 2\pi \end{aligned} \quad (80)$$

and

$$\begin{aligned} h_{11} &= \gamma_1 L \frac{E_s}{T_s}, \\ h_{12} &= 2\gamma_1 L_{12} \frac{E_s}{T_s}, \\ h_{13} &= 2\gamma_1 L_{13} \frac{E_s}{T_s}. \end{aligned} \quad (81)$$

⁹We use the convention of setting the quantities that involve a negative time index to zero.

Then by substituting in (66), we have

$$\begin{aligned} & \tilde{y}_{1,f}(jT_s + \beta_{11}L) \\ &= x_1[j] E_s e^{i\phi_1[j]} \int_0^{T_s} \frac{|p(\tau)|^2}{E_s} e^{i2\pi(v_1[j]-f)K(\tau)} d\tau. \end{aligned} \quad (82)$$

By applying Lemma 14 in Appendix D to evaluate the integral in (82), the noiseless part $\tilde{y}_{1,f}[j]$ of the output of the filter with index f at time j can be written as

$$\tilde{y}_{1,f}[j] = x_1[j] E_s e^{i\phi_1[j]} u_{1,f}[j] \quad (83)$$

where

$$u_{1,f}[j] = \begin{cases} \frac{\exp(i2\pi(v_1[j] - f)) - 1}{i2\pi(v_1[j] - f)}, & \text{if } v_1[j] \neq f \\ 1, & \text{otherwise.} \end{cases} \quad (84)$$

The output of the filter with index f at time j is

$$y_{1,f}[j] = y_{1,f}(jT_s + \beta_{11}L) = \tilde{y}_{1,f}[j] + z_{1,f}[j] \quad (85)$$

where

$$z_{1,f}[j] = z_1(t) \star h_f(t)|_{t=jT_s+\beta_{11}L}. \quad (86)$$

The variable $z_{1,f}[j]$ is Gaussian with mean 0 and variance NE_s . Moreover, due to the orthogonality of the filter bank impulse responses, we have $\mathbb{E}[z_{1,f_1}[j]z_{1,f_2}^*[j]] = 0$ for all $f_1 \neq f_2$, which implies that the random variables $\{z_{1,f}[j]\}_{f \in \mathcal{F}_1}$ are independent.

B. Discrete-Time Model

The input $x_k[j]$ of transmitter k to the channel at time j is a scalar, whereas the channel output $\mathbf{y}_k[j]$ at receiver k at time j is a vector whose components are $y_{k,f}[j]$, $f \in \mathcal{F}_k$. To compute mutual information, we now consider the codeword $\mathbf{X}_k^n = (X_k[1], X_k[2], \dots, X_k[n])$ and the receiver samples $\mathbf{Y}_k^n = (\mathbf{Y}_k[1], \mathbf{Y}_k[2], \dots, \mathbf{Y}_k[n])$ as random variables. The input-output relations are

$$Y_{k,f}[j] = X_k[j] e^{i\Phi_k[j]} U_{k,f}[j] + Z_{k,f}[j] \quad (87)$$

with

$$\begin{aligned} \Phi_1[j] &= h_{11}|X_1[j]|^2 + h_{12} \sum_{r=1}^{M_{12}} |X_2[j-r]|^2 \\ &+ h_{13} \sum_{r=1}^{M_{13}} |X_3[j-r]|^2 \end{aligned} \quad (88)$$

$$\begin{aligned} \Phi_2[j] &= h_{21} \sum_{r=1}^{M_{12}} |X_1[j+M_{12}-r]|^2 + h_{22}|X_2[j]|^2 \\ &+ h_{23} \sum_{r=1}^{M_{23}} |X_3[j-r]|^2 \end{aligned} \quad (89)$$

$$\begin{aligned} \Phi_3[j] &= h_{31} \sum_{r=1}^{M_{13}} |X_1[j+M_{13}-r]|^2 \\ &+ h_{32} \sum_{r=1}^{M_{23}} |X_2[j+M_{23}-r]|^2 + h_{33}|X_3[j]|^2 \end{aligned} \quad (90)$$

where M_{12} , M_{13} and M_{23} are positive integers and

$$U_{k,f}[j] = \begin{cases} \frac{\exp(i2\pi(V_k[j] - f)) - 1}{i2\pi(V_k[j] - f)}, & \text{if } V_k[j] \neq f \\ 1, & \text{otherwise} \end{cases} \quad (91)$$

where we define

$$\begin{aligned} V_1[j] &\triangleq h_{12}(|X_2[j]|^2 - |X_2[j-M_{12}]|^2)/2\pi \\ &+ h_{13}(|X_3[j]|^2 - |X_3[j-M_{13}]|^2)/2\pi \end{aligned} \quad (92)$$

$$\begin{aligned} V_2[j] &\triangleq h_{21}(|X_1[j+M_{12}]|^2 - |X_1[j]|^2)/2\pi \\ &+ h_{23}(|X_3[j]|^2 - |X_3[j-M_{23}]|^2)/2\pi \end{aligned} \quad (93)$$

$$\begin{aligned} V_3[j] &\triangleq h_{31}(|X_1[j+M_{13}]|^2 - |X_1[j]|^2)/2\pi \\ &+ h_{32}(|X_2[j+M_{23}]|^2 - |X_2[j]|^2)/2\pi. \end{aligned} \quad (94)$$

$Z_{k,f}[j]$ models the noise at filter f of receiver k at time j , and the random variables $\{Z_{k,f}[j]\}_{k,f,j}$ are independent circularly-symmetric complex Gaussian random variables with mean 0 and variance N . We regard the h_{kl} as *channel coefficients* that are time invariant and known globally. The following symmetric power constraints are imposed:

$$\frac{1}{n} \sum_{j=1}^n \mathbb{E}[|X_k[j]|^2] \leq P, \quad k = 1, 2, 3. \quad (95)$$

A *scheme* is a collection $\{(\mathcal{C}_1(P, N), \mathcal{C}_2(P, N), \mathcal{C}_3(P, N))\}$ of triples of codes indexed by (P, N) , such that user k uses the code $\mathcal{C}_k(P, N)$ that satisfies the power constraint and achieves an information rate $R_k(P, N)$ for $k = 1, 2, 3$ where

$$R_k(P, N) = I(X_k; \mathbf{Y}_k) \equiv \lim_{n \rightarrow \infty} \frac{1}{n} I(X_k^n; \mathbf{Y}_k^n). \quad (96)$$

We extend the definitions of pre-logs made in Definitions 1 and 2.

Definition 7: The *high-power* pre-log triple $(\bar{r}_1, \bar{r}_2, \bar{r}_3)$ is achieved by a scheme if the rates satisfy

$$\bar{r}_k(N) = \lim_{P \rightarrow \infty} \frac{R_k(P, N)}{\log(P/N)} \text{ for } k = 1, 2, 3. \quad (97)$$

Definition 8: The *low-noise* pre-log triple $(\underline{r}_1, \underline{r}_2, \underline{r}_3)$ is achieved by a scheme if the rates satisfy

$$\underline{r}_k(P) = \lim_{N \rightarrow 0} \frac{R_k(P, N)}{\log(P/N)} \text{ for } k = 1, 2, 3. \quad (98)$$

The (high-power or low-noise) pre-log triple $(1/2, 1/2, 1/2)$ can be achieved if all users use phase modulation only (see Sec. IV-C). It is not obvious whether $(1/2, 1/2, 1/2)$ is achievable by using amplitude modulation only, e.g., such as in Sec. III-B. This is because $U_{k,f}[j]$ in (87) has a random amplitude. We show in Sec. IV-D that the high-power pre-log triple $(1, 1, 1)$ can be achieved for any positive N through *interference focusing*.

C. Inner Bound: Phase Modulation

Suppose we use only the filter with index $f = 0$. Suppose further that the inputs X_k^n of user k are i.i.d. with a constant amplitude \sqrt{P} and a uniformly random phase (a ring), i.e., we have

$$X_k[j] = \sqrt{P} e^{i\Phi_{X,k}[j]} \quad (99)$$

where $\Phi_{X,k}[j]$ is uniform on $[-\pi, \pi)$ for $j = 1, 2, \dots, n$. Therefore, the outputs become

$$Y_{k,0}[j] = X_k[j] e^{i\Phi_k[j]} U_{k,0}[j] + Z_{k,0}[j] \quad (100)$$

with

$$\begin{aligned} \Phi_1[j] &= [h_{11} + h_{12}M_{12} + h_{13}M_{13}]P \\ \Phi_2[j] &= [h_{21}M_{12} + h_{22} + h_{23}M_{23}]P \\ \Phi_3[j] &= [h_{31}M_{13} + h_{32}M_{23} + h_{33}]P \end{aligned} \quad (101)$$

i.e., the phase $\Phi_k[j]$ is constant for all $j = 1, \dots, n$. Moreover, we have

$$\begin{aligned} U_{1,0}[j] &= 1, & \max\{M_{12}, M_{13}\} < j \leq n \\ U_{2,0}[j] &= 1, & M_{23} < j < n - M_{12} \\ U_{3,0}[j] &= 1, & 1 \leq j < n - \max\{M_{13}, M_{23}\}. \end{aligned} \quad (102)$$

Thus, the users are decoupled under constant amplitude modulation, except near the beginning and the end of transmission. We have

$$\begin{aligned} \frac{1}{n} I(X_1^n; \mathbf{Y}_1^n) &\stackrel{(a)}{\geq} \frac{1}{n} I(X_1^n; Y_{1,0}^n) \\ &\stackrel{(b)}{\geq} \frac{1}{n} \sum_{j=1}^n I(X_1[j]; Y_{1,0}[j]) \\ &\stackrel{(c)}{\geq} \frac{1}{n} \sum_{j=\max\{M_{12}, M_{13}\}+1}^n I(X_1[j]; Y_{1,0}[j]) \\ &\stackrel{(d)}{\geq} \left(\frac{n - \max\{M_{12}, M_{13}\}}{n} \right) \left[\frac{1}{2} \log \left(\frac{P}{N} \right) - 1 \right] \end{aligned} \quad (103)$$

where (a) follows from the chain rule and the non-negativity of mutual information, (b) follows because X_1, \dots, X_n are i.i.d. and because conditioning does not increase entropy, (c) follows from the non-negativity of mutual information and (d) holds because (see Theorem 4)

$$I(X_1[j]; Y_{1,0}[j]) \geq \frac{1}{2} \log \left(\frac{2P}{N} \right) - 1. \quad (104)$$

As $n \rightarrow \infty$, we have

$$R_1(P, N) \geq \frac{1}{2} \log \left(\frac{2P}{N} \right) - 1. \quad (105)$$

By using similar steps for users 2 and 3, we have

$$R_k(P, N) \geq \frac{1}{2} \log \left(\frac{2P}{N} \right) - 1 \quad (106)$$

for $k = 1, 2, 3$ which implies that the pre-log triple $(1/2, 1/2, 1/2)$ is achieved by using one receiver filter and phase modulation.

D. Interference Focusing

We use *interference focusing*, i.e., we focus the phase interference on *one* point by imposing the following constraints on the transmitted symbols:

$$\begin{aligned} h_{21}|X_1[j]|^2 &= 2\pi\tilde{n}_{21}, & h_{31}|X_1[j]|^2 &= 2\pi\tilde{n}_{31}, \\ h_{12}|X_2[j]|^2 &= 2\pi\tilde{n}_{12}, & h_{32}|X_2[j]|^2 &= 2\pi\tilde{n}_{32}, \\ h_{13}|X_3[j]|^2 &= 2\pi\tilde{n}_{13}, & h_{23}|X_3[j]|^2 &= 2\pi\tilde{n}_{23}, \end{aligned} \quad (107)$$

where $\tilde{n}_{21}, \tilde{n}_{31}, \tilde{n}_{12}, \tilde{n}_{32}, \tilde{n}_{13}$ and $\tilde{n}_{23} \in \mathbb{N}$, which ensures that the XPM interference is eliminated. Suppose that $h_{21}, h_{31}, h_{12}, h_{32}, h_{13}$ and h_{23} are rational. Then the interference focusing constraints become

$$|X_k[j]|^2 = 2\pi\hat{p}_k \tilde{n}_k \quad (108)$$

where

$$\hat{p}_1 \triangleq \text{lcm}(\text{den}(h_{21}), \text{den}(h_{31})), \quad (109)$$

$$\hat{p}_2 \triangleq \text{lcm}(\text{den}(h_{12}), \text{den}(h_{32})), \quad (110)$$

$$\hat{p}_3 \triangleq \text{lcm}(\text{den}(h_{13}), \text{den}(h_{23})) \quad (111)$$

where $\text{den}(x)$ is the denominator of a rational number x .

Because of the power constraint, only a subset \mathcal{P}_k of the allowed rings is actually used. In this case, $V_k[j] \in \mathcal{V}_k$, for $k = 1, 2, 3$, where

$$\mathcal{V}_k = \left\{ \sum_{j \neq k} d_j : d_j \in \mathcal{D}_j, j \in \{1, 2, 3\} \right\} \quad (112)$$

and

$$\mathcal{D}_k = \left\{ \frac{p - p'}{\hat{p}_k} : p \in \mathcal{P}_k, p' \in \mathcal{P}_k \right\} \quad (113)$$

which leads us to choose the sets of “normalized frequencies” \mathcal{F}_k of the filter banks at the receivers as $\mathcal{F}_k = \mathcal{V}_k$.

Thus, under interference focusing, the output at receiver k at time j is a vector $\mathbf{Y}_k[j]$, whose components are $\{Y_{k,f}[j]\}_{f \in \mathcal{V}_k}$, where

$$Y_{k,f}[j] = X_k[j] \exp(ih_{kk}|X_k[j]|^2) U_{k,f}[j] + Z_{k,f}[j] \quad (114)$$

and where

$$U_{k,f}[j] = \begin{cases} 1, & \text{if } V_k[j] = f, \\ 0, & \text{otherwise.} \end{cases} \quad (115)$$

This means that exactly one filter (the filter with index $V_k[j]$) output among all the filters contains the signal corrupted by noise, while all other filters put out noise. Therefore, we have

$$\begin{aligned} \frac{1}{n} I(X_k^n; \mathbf{Y}_k^n) &\stackrel{(a)}{\geq} \frac{1}{n} \sum_{j=1}^n I(X_k[j]; \mathbf{Y}_k[j]) \\ &\stackrel{(b)}{\geq} \frac{1}{n} \sum_{j=1}^n I(X_k[j]; Y_{k,V_k[j]}[j]) \\ &\stackrel{(c)}{=} I(X_k[1]; X_k[1] e^{ih_{kk}|X_k[1]|^2} + Z_{k,V_k[1]}[1]) \end{aligned} \quad (116)$$

where (a) follows because the X_k^n are i.i.d. and because conditioning does not increase entropy; (b) follows from the

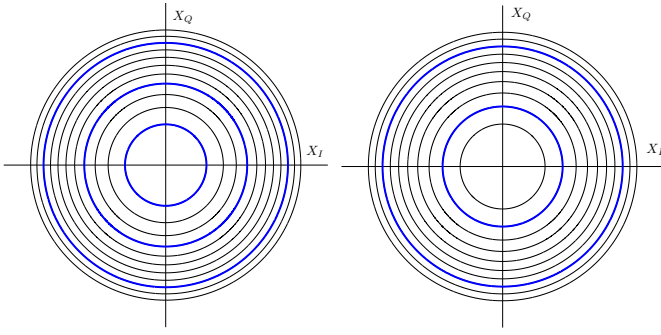


Fig. 1. Ring modulation used by transmitter 1 (left) and transmitter 2 (right). The thin lines are the rings allowed by interference focusing, and the thick blue lines are the rings selected for transmission.

chain rule and the non-negativity of mutual information (it can be shown that equality holds, see Appendix E); and (c) holds because the X_k^n are i.i.d. and the channel becomes a memoryless time-invariant channel under interference focusing. It follows from Theorem 5 that by using interference focusing, we have

$$\lim_{P \rightarrow \infty} \frac{I(X_k[1]; X_k[1]e^{ih_{kk}|X_k[1]|^2} + Z_{k,V_k[1]}[1])}{\log(P/N)} \geq 1 \quad (117)$$

which implies that $\bar{r}_k \geq 1$ for $k = 1, 2, 3$. Hence, the high-power pre-log triple $(1, 1, 1)$ is achievable. We again remark that the above analysis generalizes for different power constraints at the transmitters. However, the question of whether all users can simultaneously achieve a low-noise pre-log of 1 is open for both models with and without GVM.

The following (downsized) example illustrates our receiver structure, and the role that interference focusing plays in choosing its parameters.

Example: Consider 2 transmitters that use a rectangular pulse, i.e., suppose

$$p(t) = \begin{cases} \sqrt{E_s/T_s}, & 0 \leq t < T_s \\ 0, & \text{otherwise} \end{cases} \quad (118)$$

where the power constraints are $P_1 = 8$ and $P_2 = 7$ on transmitter 1 and 2, respectively. Suppose that $h_{12} = 5$, $h_{21} = 4$. Since this is a two-user system, we may use (34) and (35) rather than (109) and (110), i.e., we use $\hat{p}_1 = 1/h_{21} = 0.25$ and $\hat{p}_2 = 1/h_{12} = 0.2$. Suppose that the users choose the power levels $\mathcal{P}_1 = \{2\pi\hat{p}_1\tilde{n}_1 : \tilde{n}_1 = 1, 4, 9\} = \{0.5\pi, 2\pi, 4.5\pi\}$ and $\mathcal{P}_2 = \{2\pi\hat{p}_2\tilde{n}_2 : \tilde{n}_2 = 2, 8\} = \{0.8\pi, 3.2\pi\}$ (see Fig. 1). These choices satisfy the power constraints and eliminate the interference. The parameters of the filter banks are $\mathcal{F}_1 = \mathcal{V}_1 = \{-6, 0, 6\}$ and $\mathcal{F}_2 = \mathcal{V}_2 = \{-8, -5, -3, 0, 3, 5, 8\}$. In other words, receiver 1 has 3 filters whose frequency responses are sinc functions centered at $f_1 - 6/T_s$, f_1 , and $f_1 + 6/T_s$, whereas receiver 2 has 7 filters whose frequency responses are sinc functions centered at 7 different frequencies (see Fig. 2). This shows that, because of the nonlinearity, the receivers need to extract information from a “bandwidth” larger than the “bandwidth” of the transmitted signal.

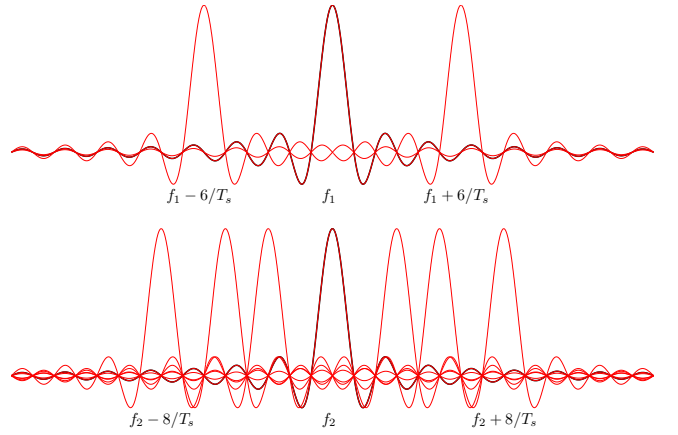


Fig. 2. Frequency responses of the filters at receivers 1 (top) and 2 (bottom).

E. Outer Bound

1) *Interference Focusing:* We show next that the maximal pre-log triple for the model of Sec. IV-B is $(1, 1, 1)$ when interference focusing is used. We have

$$\begin{aligned} I(X_1^n; \mathbf{Y}_1^n) &\stackrel{(a)}{\leq} I(X_1^n; \mathbf{Y}_1^n, V_1^n) \\ &\stackrel{(b)}{=} I(X_1^n; \mathbf{Y}_1^n | V_1^n) \\ &\stackrel{(c)}{=} I(X_1^n; Y_{1,V_1[1]} Y_{1,V_1[2]} \dots Y_{1,V_1[n]} | V_1^n) \\ &\stackrel{(d)}{=} I(X_1^n; Y_{1,V_1[1]} Y_{1,V_1[2]} \dots Y_{1,V_1[n]}) \\ &\leq n \log \left(1 + \frac{P}{N} \right). \end{aligned} \quad (119)$$

Step (a) follows from the chain rule and the non-negativity of mutual information; (b) holds because X_1^n is independent of V_1^n ; (c) holds because $Y_{1,f}[j] = Z_{1,f}[j]$ for $f \neq V_1[j]$ and the variables $\{Z_{1,f}[j] : j = 1, \dots, n \text{ and } f \neq V_1[j]\}$ are independent of $Y_{1,V_1[1]}, Y_{1,V_1[2]}, \dots, Y_{1,V_1[n]}$ and X_1^n and (d) holds because X_1^n and $Y_{1,V_1[1]}, Y_{1,V_1[2]}, \dots, Y_{1,V_1[n]}$ are independent of V_1^n (which follows from $Z_{1,V_1[1]}, Z_{1,V_1[2]}, \dots, Z_{1,V_1[n]}$ being i.i.d.). By using a similar argument for receiver 2 and receiver 3, we eventually have

$$R_k \leq \log \left(1 + \frac{P}{N} \right) \quad (120)$$

for $k = 1, 2, 3$ which implies that the maximal pre-log triple is $(1, 1, 1)$.

2) *General Modulation:* We show next that the maximal pre-log triple is $(1, 1, 1)$ for any modulation scheme. We use a genie-aided strategy. Suppose a genie reveals the codewords x_2^n and x_3^n of users 2 and 3 to receiver 1 prior to transmission. Receiver 1 generates $\phi_{12}(t)$ and $\phi_{13}(t)$ according to (69) and (70), respectively, and uses them to cancel XPM in the received signal, i.e., receiver 1 generates

$$\tilde{r}_1(t) = r_1(t) e^{-j\phi_{12}(t) - j\phi_{13}(t)}. \quad (121)$$

The XPM-free signal $\tilde{r}(t)$ is fed to a filter with an impulse response $p^*(-t)$ and the output of the filter is sampled at symbol rate. Matched filtering with symbol rate sampling does

not incur any information loss because XPM is canceled. The j -th filter output is

$$\begin{aligned}\tilde{y}_1[j] &= \tilde{r}_1(t) \star p^*(-t)|_{t=jT_s} \\ &= x_1[j]e^{j h_{11}|x_1[j]|^2} + \tilde{z}_1[j]\end{aligned}\quad (122)$$

where $\tilde{z}_1[j]$ is a realization of a Gaussian random variable with mean zero and variance N . The channel (122) is a memoryless AWGN channel and therefore we have

$$I(X_1^n; \tilde{Y}_1[1]\tilde{Y}_1[2]\dots\tilde{Y}_1[n]) \leq n \log \left(1 + \frac{P}{N}\right). \quad (123)$$

Similarly, it can be shown that the maximum pre-log for users 2 and 3 is 1, implying that the maximal pre-log triple is $(1, 1, 1)$.

V. DISCUSSION

Interference focusing is reminiscent of interference alignment, which refers to techniques of signal construction so that undesired signals at each receiver arrive along the same dimensions while the desired signal can be resolved through the remaining dimensions. We highlight the main differences between interference alignment and interference focusing.

Cadambe and Jafar [42] introduced an (asymptotic) interference alignment scheme for K -user single-input single-output linear interference channels which achieves the optimal degrees of freedom (DoF) as long as the channel coefficients are time-varying (or frequency-selective). Their scheme relies on beamforming over symbol extensions to separate signal spaces based on linear independence.

For constant channels, especially with real channel coefficients, interference alignment along linearly independent dimensions may not achieve the optimal DoF. Motahari et al [43] developed interference alignment along rationally independent dimensions to achieve the optimal DoF. Their approach is referred to as *real* interference alignment.

Interference alignment lets each user achieve half the DoF that can be achieved in the absence of all other interferers (colloquially: each user gets half “the cake”). In contrast, orthogonalization techniques, e.g., time division or frequency division, split the resources among K users so that each user gets only $1/K$ of the resources.

In optical fiber, splitting the bandwidth among K users by using WDM does not guarantee that each user gets $1/K$ of the interference-free capacity (IFC) because of the fiber nonlinearity. In the zero-dispersion case, for example, each user gets $1/(2K)$ of the IFC using Gaussian modulation. We have shown interference focusing enables each user to get $1/K$ of the IFC, but not half of it, at high SNR. We remark that interference focusing requires neither symbol extensions nor global CSI.

VI. CONCLUSION

We introduced two discrete-time interference channel models based on a simplified optical fiber model. We used coupled differential equations derived from the NLS equation to develop our models. In the first model, there was no dispersion. This discrete-time model was justified by using

a rectangular pulse shape at the transmitters and matched filters at the receivers. The nonlinear nature of the fiber-optic medium causes the users to suffer from amplitude-dependent phase interference. We introduced a new technique called interference focusing that lets the users take advantage of all the available amplitude and phase degrees of freedom at high transmission powers. In the second model, the second-order dispersion is negligible. However, we included non-zero GVM as well as nonlinearity. We justified this discrete-time model by using a time-limited pulse shape at the transmitters and a bank of “frequency-shifted” matched filters at each receiver. We proved that all users can achieve a high-power pre-log of 1 simultaneously by using interference focusing. We also showed that interference focusing is optimal (for the model of Sec. IV-B) in the pre-log sense.

APPENDIX A

UPPER BOUND ON THE MODIFIED BESSEL FUNCTION OF THE FIRST KIND OF ORDER ZERO

Lemma 9:

$$I_0(z) \leq \frac{e^z}{\sqrt{z}}, \quad z > 0 \quad (124)$$

Proof: We have

$$\cos \theta \leq 1 - 4\theta^2/\pi^2, \quad 0 \leq \theta \leq \pi/2 \quad (125)$$

$$\cos \theta \leq 0, \quad \pi/2 \leq \theta \leq \pi \quad (126)$$

where (125) follows by the infinite product form

$$\cos x = \prod_{n=1}^{\infty} \left[1 - \frac{4x^2}{\pi^2(2n-1)^2}\right]. \quad (127)$$

We thus have

$$\begin{aligned}I_0(z) &= \frac{1}{\pi} \int_0^{\pi} e^{z \cos \theta} d\theta \\ &\stackrel{(a)}{\leq} \frac{1}{\pi} \left[\int_0^{\pi/2} e^{z(1-4\theta^2/\pi^2)} d\theta + \int_{\pi/2}^{\pi} d\theta \right] \\ &= \frac{\sqrt{\pi}}{4} \frac{e^z}{\sqrt{z}} \left(1 - 2Q(\sqrt{2z})\right) + \frac{1}{2} \\ &\stackrel{(b)}{\leq} \frac{\sqrt{\pi}}{2} \frac{e^z}{\sqrt{z}} \\ &\leq \frac{e^z}{\sqrt{z}}\end{aligned}\quad (128)$$

where

$$Q(z) = \int_z^{\infty} \frac{1}{\sqrt{2\pi}} e^{-x^2/2} dx. \quad (129)$$

Step (a) follows because the exponential function is a monotonic increasing function and by (125)–(126), while (b) holds because $Q(z) \geq 0$ and

$$\frac{\sqrt{\pi}}{4} \frac{e^z}{\sqrt{z}} \geq \frac{\sqrt{\pi}}{4} \min_{z \geq 0} \frac{e^z}{\sqrt{z}} = \frac{\sqrt{2e\pi}}{4} \geq \frac{1}{2}. \quad (130)$$

■

APPENDIX B

EXPECTED VALUE OF THE LOGARITHM OF A RICIAN R.V.

Consider the following functions.

- Gamma function $\Gamma(z)$ [44, 6.1.1]

$$\Gamma(z) = \int_0^\infty t^{z-1} e^{-t} dt \quad (131)$$

- Psi (Digamma) function $\psi(z)$ [44, 6.3.1]

$$\psi(z) = \frac{d}{dz} \ln \Gamma(z) = \frac{\Gamma'(z)}{\Gamma(z)} \quad (132)$$

- Upper incomplete Gamma function $\Gamma(a, x)$ [44, 6.5.3]

$$\Gamma(a, x) = \int_x^\infty t^{a-1} e^{-t} dt, \quad a > 0 \quad (133)$$

We derive several useful lemmas concerning these functions.

Lemma 10:

$$\int_0^\infty e^{-\frac{x^2}{2}} x^{2k+1} \ln(x) dx = 2^{k-1} (\Gamma(k+1) \ln(2) + \Gamma'(k+1)) \quad (134)$$

Proof: Consider

$$\begin{aligned} \mathcal{I}_k &\triangleq \int_0^\infty e^{-\frac{x^2}{2}} x^{2k+1} \ln(x) dx \\ &\stackrel{(a)}{=} \int_0^\infty e^{-u} (\sqrt{2u})^{2k+1} \ln(\sqrt{2u}) \frac{1}{\sqrt{2u}} du \\ &= \int_0^\infty e^{-u} (2u)^k \frac{1}{2} (\ln(2) + \ln(u)) du \\ &= 2^{k-1} \ln(2) \int_0^\infty e^{-u} u^k du + 2^{k-1} \int_0^\infty e^{-u} u^k \ln(u) du \\ &\stackrel{(b)}{=} 2^{k-1} (\Gamma(k+1) \ln(2) + \Gamma'(k+1)) \end{aligned} \quad (135)$$

where (a) follows from the transformation of variables $u = x^2/2$ and (b) follows by (131) and [45, 4.352 (4)]

$$\int_{u=0}^\infty e^{-u} u^k \ln(u) du = \Gamma'(k+1). \quad (136)$$

Lemma 11:

$$\sum_{k=0}^\infty \frac{t^k}{k!} \psi(k+1) = e^t (\Gamma(0, t) + \ln(t)) \quad (137)$$

Proof: We use the following formula [46, 6.2.1 (60)]

$$\begin{aligned} \sum_{k=1}^\infty \frac{t^k}{k!} \psi(k+a) &= \frac{t}{a} e^t \left[a \psi(a) \frac{1-e^{-t}}{t} \right. \\ &\quad \left. + {}_2F_2(1, 1; a+1, 2; -t) \right] \end{aligned} \quad (138)$$

where ${}_2F_2(a_1, a_2; b_1, b_2; x)$ is the generalized hypergeometric function defined as [45, 9.14 (1)], [46, p. 674]

$${}_2F_2(a_1, a_2; b_1, b_2; x) = \sum_{k=0}^\infty \frac{(a_1)_k (a_2)_k}{(b_1)_k (b_2)_k} \frac{x^k}{k!} \quad (139)$$

where $(f)_k \triangleq f(f+1) \dots (f+k-1)$. Setting $a = 1$ in (138) gives

$$\begin{aligned} \sum_{k=1}^\infty \frac{t^k}{k!} \psi(k+1) &= t e^t \left[\psi(1) \frac{1-e^{-t}}{t} + {}_2F_2(1, 1; 2, 2; -t) \right] \\ &= e^t [F(t) + (1-e^{-t})\psi(1)] \end{aligned} \quad (140)$$

where we defined $F(t)$ as

$$\begin{aligned} F(t) &\triangleq t \cdot {}_2F_2(1, 1; 2, 2; -t) \\ &= t \sum_{k=0}^\infty \frac{1}{(k+1)^2} \frac{(-t)^k}{k!} \\ &= \sum_{m=1}^\infty \frac{-1}{m} \frac{(-t)^m}{m!}. \end{aligned} \quad (141)$$

From the Fundamental Theorem of Calculus, we have

$$\int_0^z F'(t) dt = F(z) - F(0) \quad (142)$$

where

$$F'(t) \triangleq \frac{dF(t)}{dt} = \sum_{m=1}^\infty \frac{(-t)^{m-1}}{m!} = \frac{1-e^{-t}}{t} \quad (143)$$

and therefore the left-hand side of (142) is

$$\begin{aligned} \int_0^z \frac{1-e^{-t}}{t} dt &= \int_z^\infty \frac{e^{-t}}{t} dt + \int_1^z \frac{1}{t} dt \\ &\quad + \left(\int_0^1 \frac{1-e^{-t}}{t} dt - \int_1^\infty \frac{e^{-t}}{t} dt \right) \\ &= \Gamma(0, z) + \ln(z) + \gamma \end{aligned} \quad (144)$$

where we used the definition of the upper incomplete Gamma function and the following integral form for Euler's constant [45, 8.367 (12)]

$$\gamma = \int_0^1 \frac{1-e^{-t}}{t} dt - \int_1^\infty \frac{e^{-t}}{t} dt. \quad (145)$$

Since $F(0) = 0$ and $\psi(1) = -\gamma$ [45, 8.367 (1)], we have

$$F(z) = \Gamma(0, z) + \ln(z) - \psi(1). \quad (146)$$

The lemma follows from (140) and (146). ■

Lemma 12:

$$\int_0^\infty x e^{-\frac{x^2+\nu^2}{2}} I_0(x\nu) \ln(x) dx = \frac{1}{2} \left(\Gamma\left(0, \frac{\nu^2}{2}\right) + \ln(\nu^2) \right) \quad (147)$$

Proof: We compute

$$\begin{aligned}
& \int_0^\infty x e^{-\frac{x^2+\nu^2}{2}} I_0(x\nu) \ln(x) dx \\
& \stackrel{(a)}{=} \int_0^\infty x e^{-\frac{x^2+\nu^2}{2}} \left(\sum_{k=0}^\infty \frac{(x^2\nu^2/4)^k}{(k!)^2} \right) \ln(x) dx \\
& = \sum_{k=0}^\infty \frac{1}{4^k (k!)^2} \left(\int_0^\infty x e^{-\frac{x^2+\nu^2}{2}} (x\nu)^{2k} \ln(x) dx \right) \\
& \stackrel{(b)}{=} \sum_{k=0}^\infty \frac{1}{4^k (k!)^2} 2^{k-1} e^{-\frac{\nu^2}{2}} \nu^{2k} (\Gamma(k+1) \ln(2) + \Gamma'(k+1)) \\
& \stackrel{(c)}{=} e^{-\frac{\nu^2}{2}} \left[\frac{\ln(2)}{2} \sum_{k=0}^\infty \frac{(\nu^2/2)^k}{k!} + \frac{1}{2} \sum_{k=0}^\infty \frac{(\nu^2/2)^k}{k!} \psi(k+1) \right] \\
& \stackrel{(d)}{=} e^{-\frac{\nu^2}{2}} \left[\frac{\ln(2)}{2} e^{\frac{\nu^2}{2}} + \frac{1}{2} e^{\frac{\nu^2}{2}} \left(\Gamma\left(0, \frac{\nu^2}{2}\right) + \ln\left(\frac{\nu^2}{2}\right) \right) \right] \\
& = \frac{1}{2} \left(\Gamma\left(0, \frac{\nu^2}{2}\right) + \ln(\nu^2) \right) \tag{148}
\end{aligned}$$

where in (a) we used the series representation of $I_0(\cdot)$ [44, 9.6.10]

$$I_0(x) = \sum_{k=0}^\infty \frac{(x^2/4)^k}{(k!)^2}. \tag{149}$$

Step (b) follows from Lemma 10, (c) follows because [44, 6.1.6]

$$\Gamma(k+1) = k! \tag{150}$$

and $\psi(k+1) = \Gamma'(k+1)/\Gamma(k+1)$ and (d) follows by Lemma 11. ■

APPENDIX C MINIMUM-DISTANCE ESTIMATOR

Let $Y = X + Z$ where Z is a circularly-symmetric complex Gaussian random variable with mean 0 and variance N . Suppose $X_A \triangleq |X| \in \mathcal{X}_A = \{\sqrt{\mathbf{P}_j} : j = 1, \dots, J\}$ where $0 < \mathbf{P}_1 < \mathbf{P}_2 < \dots < \mathbf{P}_J$. Define the minimum-distance estimator \hat{X}_A as

$$\hat{X}_A = \arg \min_{x_A \in \mathcal{X}_A} |Y_A - x_A| \tag{151}$$

where $Y_A = |Y|$.

Lemma 13: The probability of error for uniformly distributed X_A satisfies

$$P_e \triangleq \Pr[\hat{X}_A \neq X_A] \leq \frac{2}{J} \sum_{j=2}^J \exp\left(-\frac{\Delta_j^2}{4}\right) \tag{152}$$

where $\Delta_j = (\sqrt{\mathbf{P}_j} - \sqrt{\mathbf{P}_{j-1}})/\sqrt{N}$.

Proof: Let $P_{e,j}$ be the error probability when $X_A =$

$\sqrt{\mathbf{P}_j}$. We have $P_e = \sum_{j=1}^J (1/J) P_{e,j}$ and

$$P_{e,j} = \begin{cases} \Pr\left(Y_A \geq \frac{\sqrt{\mathbf{P}_1} + \sqrt{\mathbf{P}_2}}{2}\right), & j = 1 \\ \Pr\left(Y_A \leq \frac{\sqrt{\mathbf{P}_{K-1}} + \sqrt{\mathbf{P}_K}}{2}\right), & j = J \\ \Pr\left(Y_A \leq \frac{\sqrt{\mathbf{P}_{j-1}} + \sqrt{\mathbf{P}_j}}{2}\right) \\ + \Pr\left(Y_A \geq \frac{\sqrt{\mathbf{P}_j} + \sqrt{\mathbf{P}_{j+1}}}{2}\right), & \text{otherwise.} \end{cases} \tag{153}$$

Conditioned on $X_A = \sqrt{\mathbf{P}_j}$, Y_A is a Ricean random variable, and hence we compute [47, p. 50]

$$\Pr\left(Y_A \geq \frac{\sqrt{\mathbf{P}_j} + \sqrt{\mathbf{P}_{j+1}}}{2}\right) = Q\left(\frac{\sqrt{\mathbf{P}_j}}{\sqrt{N/2}}, \frac{\sqrt{\mathbf{P}_j} + \sqrt{\mathbf{P}_{j+1}}}{2\sqrt{N/2}}\right) \tag{154}$$

where $Q(a, b)$ is the Marcum Q-function [48]. Consider the following bounds.

- Upper bound for $b > a$ [48, UB1MG]

$$Q(a, b) \leq \exp\left(-\frac{(b-a)^2}{2}\right). \tag{155}$$

- Lower bound for $b < a$ [48, LB2aS]

$$\begin{aligned}
& Q(a, b) \\
& \geq 1 - \frac{1}{2} \left[\exp\left(-\frac{(a-b)^2}{2}\right) - \exp\left(-\frac{(a+b)^2}{2}\right) \right]. \tag{156}
\end{aligned}$$

The bound (156) implies

$$1 - Q(a, b) \leq \exp\left(-\frac{(a-b)^2}{2}\right). \tag{157}$$

We use (154) and (155) to write

$$\Pr\left(Y_A \geq \frac{\sqrt{\mathbf{P}_j} + \sqrt{\mathbf{P}_{j+1}}}{2}\right) \leq \exp\left(-\frac{\Delta_{j+1}^2}{4}\right). \tag{158}$$

where $\Delta_j = (\sqrt{\mathbf{P}_j} - \sqrt{\mathbf{P}_{j-1}})/\sqrt{N}$. Similarly, we use inequality (157) to write

$$\Pr\left(Y_A \leq \frac{\sqrt{\mathbf{P}_{j-1}} + \sqrt{\mathbf{P}_j}}{2}\right) \leq \exp\left(-\frac{\Delta_j^2}{4}\right). \tag{159}$$

Collecting our results, we have

$$\begin{aligned}
P_e & \leq \frac{1}{J} \left[\exp\left(-\frac{\Delta_2^2}{4}\right) + \sum_{j=2}^{J-1} \exp\left(-\frac{\Delta_j^2}{4}\right) \right. \\
& \quad \left. + \sum_{j=2}^{J-1} \exp\left(-\frac{\Delta_{j+1}^2}{4}\right) + \exp\left(-\frac{\Delta_J^2}{4}\right) \right] \\
& = \frac{2}{J} \sum_{j=2}^J \exp\left(-\frac{\Delta_j^2}{4}\right). \tag{160}
\end{aligned}$$

■

APPENDIX D ORTHOGONALITY OF IMPULSE RESPONSES

We introduce a useful lemma.

Lemma 14: For any complex number B , we have

$$\int_0^{T_s} \frac{|p(t)|^2}{E_s} e^{BK(\tau)} d\tau = \begin{cases} (e^B - 1)/B, & \text{if } B \neq 0, \\ 1, & \text{if } B = 0 \end{cases} \quad (161)$$

where $K(\cdot)$ is defined in (62).

Proof:

- For $B = 0$, we have

$$\int_0^{T_s} \frac{|p(t)|^2}{E_s} e^{BK(\tau)} d\tau = \int_0^{T_s} \frac{|p(t)|^2}{E_s} d\tau = 1 \quad (162)$$

where the last equality follows from (16).

- For $B \neq 0$, we have

$$\begin{aligned} \int_0^{T_s} \frac{|p(t)|^2}{E_s} e^{BK(\tau)} d\tau &\stackrel{(a)}{=} \frac{1}{B} \int_0^{T_s} BK'(\tau) e^{BK(\tau)} d\tau \\ &\stackrel{(b)}{=} \frac{e^{BK(T_s)} - e^{BK(0)}}{B} \\ &\stackrel{(c)}{=} \frac{e^B - 1}{B} \end{aligned} \quad (163)$$

where (a) follows by applying Leibniz's theorem for differentiation of an integral [44, 3.3.7]:

$$K'(t) = \frac{1}{E_s} \frac{d}{dt} \int_0^t |p(\lambda)|^2 d\lambda = \frac{1}{E_s} |p(t)|^2; \quad (164)$$

(b) is obtained through integration by substitution and (c) holds because $K(0) = 0$ and $K(T_s) = 1$. ■

Next we show that the impulse responses $\{h_f(t)\}_{f \in \mathcal{F}_1}$ are orthogonal (cf. (63)). For $f_1 \neq f_2$, we have

$$\begin{aligned} &\int_{-\infty}^{\infty} h_{f_1}(\xi) h_{f_2}^*(\xi) d\xi \\ &\stackrel{(a)}{=} \int_{-\infty}^{\infty} |p(-\xi)|^2 \exp(-i2\pi(f_1 - f_2)K(-\xi)) d\xi \\ &\stackrel{(b)}{=} \int_{-\infty}^{\infty} |p(t)|^2 \exp(-i2\pi(f_1 - f_2)K(t)) dt \\ &\stackrel{(c)}{=} \int_0^{T_s} |p(t)|^2 \exp(-i2\pi(f_1 - f_2)K(t)) dt \\ &\stackrel{(d)}{=} 0 \end{aligned} \quad (165)$$

where (a) follows from $K^*(\xi) = K(\xi)$, (b) follows from the transformation of variables $t = -\xi$, (c) holds because $p(t) = 0$ for $t \notin [0, T_s]$ and (d) follows from Lemma 14 with $B = -i2\pi(f_1 - f_2) \neq 0$.

APPENDIX E INDEPENDENCE OF FILTER OUTPUTS

We drop the user index and time index for notational simplicity. We decompose \mathbf{Y} into Y_V and $\bar{\mathbf{Y}}_V$ where $\bar{\mathbf{Y}}_V =$

$(Y_q : q \in \mathcal{V} \setminus \{V\})$. Let $\bar{\mathbf{y}} = (\tilde{y}_q : q = 1, \dots, |\mathcal{V}| - 1) \in \mathbb{C}^{|\mathcal{V}| - 1}$. The joint pdf of X , Y_V and $\bar{\mathbf{Y}}_V$ is

$$\begin{aligned} p_{X, Y_V, \bar{\mathbf{Y}}_V}(x, y, \bar{\mathbf{y}}) &= p_X(x) \sum_{v \in \mathcal{V}} p_{Y_V, \bar{\mathbf{Y}}_V, V|X}(y, \bar{\mathbf{y}}, v|x) \\ &= p_X(x) \sum_{v \in \mathcal{V}} p_V(v) p_Z(y - x) \prod_{q=1}^{|\mathcal{V}|-1} p_Z(\tilde{y}_q) \\ &= p_X(x) p_Z(y - x) \prod_{q=1}^{|\mathcal{V}|-1} p_Z(\tilde{y}_q) \\ &= p_X(x) p_{Y_V|X}(y|x) p_{\bar{\mathbf{Y}}_V}(\bar{\mathbf{y}}). \end{aligned} \quad (166)$$

where $p_Z(\cdot)$ is the pdf of Z_f for $f \in \mathcal{V}$ and is given by

$$p_Z(z) \triangleq \frac{1}{\pi N} e^{-|z|^2/N}. \quad (167)$$

Therefore, we find that X and Y_V are statistically independent of $\bar{\mathbf{Y}}_V$ and

$$I(X; \bar{\mathbf{Y}}_V | Y_V) = 0. \quad (168)$$

Hence, we have

$$I(X; \mathbf{Y}) = I(X; Y_V) + I(X; \bar{\mathbf{Y}}_V | Y_V) = I(X; Y_V). \quad (169)$$

ACKNOWLEDGEMENT

We thank the reviewers and the Associate Editor for useful comments.

REFERENCES

- [1] R.-J. Essiambre, G. Kramer, P. J. Winzer, G. Foschini, and B. Goebel, "Capacity limits of optical fiber networks," *J. Lightw. Technol.*, vol. 28, no. 4, pp. 662–701, Feb. 2010.
- [2] A. Splett, C. Kurtzke, and K. Petermann, "Ultimate transmission capacity of amplified optical fiber communication systems taking into account fiber nonlinearities," in *Euro. Conf. Opt. Commun. (ECOC)*, Montreux, Switzerland, Sep. 1993, pp. 41–44.
- [3] E. Narimanov and P. Mitra, "The Channel Capacity of a Fiber Optics Communication System: Perturbation Theory," *J. Lightw. Technol.*, vol. 20, no. 3, pp. 530–537, Mar. 2002.
- [4] L. Xiang and X. P. Zhang, "The study of information capacity in multi-span nonlinear optical fiber communication systems using a developed perturbation technique," *J. Lightw. Technol.*, vol. 29, no. 3, pp. 260–264, Feb. 2011.
- [5] A. Mecozzi, "Limits to long-haul coherent transmission set by the Kerr nonlinearity and noise of the in-line amplifiers," *J. Lightw. Technol.*, vol. 12, no. 11, pp. 1993–2000, Nov. 1994.
- [6] K. Turitsyn, S. Derevyanko, I. Yurkevich, and S. Turitsyn, "Information capacity of optical fiber channels with zero average dispersion," *Phys. Rev. Lett.*, vol. 91, p. 203901, Nov. 2003.
- [7] M. Yousefi and F. Kschischang, "A probabilistic model for optical fiber channels with zero dispersion," in *Biennial Symp. Commun. (QBSC)*, Kingston, ON, Canada, May 2010, pp. 221–225.
- [8] —, "A Fokker-Planck differential equation approach for the zero-dispersion optical fiber channel," in *IEEE Int. Symp. Inf. Theory (ISIT)*, Austin, TX, Jun. 2010, pp. 206–210.
- [9] —, "On the per-sample capacity of nondispersive optical fibers," *IEEE Trans. Inf. Theory*, vol. 57, no. 11, pp. 7522–7541, Nov. 2011.
- [10] H. Wei and D. Plant, "Comment on 'Information capacity of optical fiber channels with zero average dispersion'," *ArXiv Physics e-prints*, 2006.
- [11] P. P. Mitra and J. B. Stark, "Nonlinear limits to the information capacity of optical fibre communications," *Nature*, vol. 411, pp. 1027–1039, Jun. 2001.

- [12] J. Tang, "The Shannon channel capacity of dispersion-free nonlinear optical fiber transmission," *J. Lightw. Technol.*, vol. 19, no. 8, pp. 1104–1109, Aug. 2001.
- [13] I. Djordjevic, B. Vasic, M. Ivkovic, and I. Gabitov, "Achievable information rates for high-speed long-haul optical transmission," *J. Lightw. Technol.*, vol. 23, no. 11, pp. 3755–3763, Nov. 2005.
- [14] M. Ivkovic, I. Djordjevic, and B. Vasic, "Calculation of achievable information rates of long-haul optical transmission systems using instanton approach," *J. Lightw. Technol.*, vol. 25, no. 5, pp. 1163–1168, May 2007.
- [15] L. Wegener, M. Povinelli, A. Green, P. Mitra, J. Stark, and P. Littlewood, "The effect of propagation nonlinearities on the information capacity of WDM optical fiber systems: cross-phase modulation and four-wave mixing," *Physica D: Nonlinear Phenomena*, vol. 189, no. 1-2, pp. 81–99, Feb. 2004.
- [16] K.-P. Ho and J. Kahn, "Channel capacity of WDM systems using constant-intensity modulation formats," in *Opt. Fiber Commun. Conf. (OFC)*, Anaheim, CA, USA, Mar. 2002, pp. 731–733.
- [17] J. Tang, "The multispan effects of Kerr nonlinearity and amplifier noises on Shannon channel capacity of a dispersion-free nonlinear optical fiber," *J. Lightw. Technol.*, vol. 19, no. 8, pp. 1110–1115, Aug. 2001.
- [18] —, "The channel capacity of a multispan DWDM system employing dispersive nonlinear optical fibers and an ideal coherent optical receiver," *J. Lightw. Technol.*, vol. 20, no. 7, pp. 1095–1101, Jul. 2002.
- [19] K. Peddanarappagari and M. Brandt-Pearce, "Volterra series transfer function of single-mode fibers," *J. Lightw. Technol.*, vol. 15, no. 12, pp. 2232–2241, Dec. 1997.
- [20] M. Taghavi, G. Papan, and P. Siegel, "On the multiuser capacity of WDM in a nonlinear optical fiber: Coherent communication," *IEEE Trans. Inf. Theory*, vol. 52, no. 11, pp. 5008–5022, Oct. 2006.
- [21] G. Bosco, P. Poggiolini, A. Carena, V. Curri, and F. Forghieri, "Analytical results on channel capacity in uncompensated optical links with coherent detection," *Opt. Express*, vol. 19, no. 26, pp. B440–B451, Dec. 2011.
- [22] —, "Analytical results on channel capacity in uncompensated optical links with coherent detection: erratum," *Opt. Express*, vol. 20, no. 17, pp. 19610–19611, Aug. 2012.
- [23] P. Poggiolini, "The GN model of non-linear propagation in uncompensated coherent optical systems," *J. Lightw. Technol.*, vol. 30, no. 24, pp. 3857–3879, Dec. 2012.
- [24] A. Mecozzi and R. Essiambre, "Nonlinear Shannon limit in pseudolinear coherent systems," *J. Lightw. Technol.*, vol. 30, no. 12, pp. 2011–2024, Jun. 2012.
- [25] M. Secondini, E. Forestieri, and G. Prati, "Achievable information rate in nonlinear WDM fiber-optic systems with arbitrary modulation formats and dispersion maps," *J. Lightw. Technol.*, vol. 31, no. 23, pp. 3839–3852, Dec. 2013.
- [26] R. Dar, M. Shtaf, and M. Feder, "Information rates in the optical nonlinear phase-noise channel," in *Annu. Allerton Conf. Commun. Control. and Comput.*, Oct. 2013.
- [27] —, "New bounds on the capacity of the nonlinear fiber-optic channel," *Opt. Lett.*, vol. 39, no. 2, pp. 398–401, Jan. 2014.
- [28] —, "Improved bounds on the nonlinear fiber-channel capacity," in *Euro. Conf. Opt. Commun. (ECOC)*, London, UK, Sep. 2013, pp. 1–3.
- [29] E. Agrell, A. Alvarado, G. Durisi, and M. Karlsson, "Capacity of a nonlinear optical channel with finite memory," *J. Lightw. Technol.*, vol. 32, no. 16, pp. 2862–2876, Aug. 2014.
- [30] M. Yousefi and F. Kschischang, "Integrable communication channels and the nonlinear Fourier transform," in *IEEE Int. Symp. Inf. Theory (ISIT)*, Istanbul, Turkey, Jul. 2013, pp. 1705–1709.
- [31] —, "Communication over fiber-optic channels using the nonlinear Fourier transform," in *IEEE Int. Symp. Inf. Theory (ISIT)*, Istanbul, Turkey, Jul. 2013, pp. 1710–1714.
- [32] —, "Information transmission using the nonlinear Fourier transform, Part I: Mathematical tools," *IEEE Trans. Inf. Theory*, vol. 60, no. 7, pp. 4312–4328, Jul. 2014.
- [33] —, "Information transmission using the nonlinear Fourier transform, Part II: Numerical methods," *IEEE Trans. Inf. Theory*, vol. 60, no. 7, pp. 4329–4345, Jul. 2014.
- [34] —, "Information transmission using the nonlinear Fourier transform, Part III: Spectrum modulation," *IEEE Trans. Inf. Theory*, vol. 60, no. 7, pp. 4346–4369, Jul. 2014.
- [35] H. Ghazlan and G. Kramer, "Interference focusing for mitigating cross-phase modulation in a simplified optical fiber model," in *IEEE Int. Symp. Inf. Theory (ISIT)*, Austin, TX, Jun. 2010, pp. 2033–2037.
- [36] —, "Interference focusing for simplified optical fiber models with dispersion," in *IEEE Int. Symp. Inf. Theory (ISIT)*, St. Petersburg, Russia, Aug. 2011, pp. 376–379.
- [37] G. P. Agrawal, *Nonlinear Fiber Optics*, 3rd ed. Academic Press, 2001.
- [38] H. Ghazlan, *Models and information rates for channels with nonlinearity and phase noise*. Ph.D. Dissertation, Dept. Elect. Eng., Univ. Southern California, Los Angeles, CA, USA, 2015.
- [39] A. Lapidot, "Capacity bounds via duality: A phase noise example," in *Asian-Euro. Workshop Inf. Theory*, Breisach, Germany, Jun. 2002, pp. 58–61.
- [40] R.-J. Essiambre, G. Foschini, G. Kramer, and P. Winzer, "Capacity limits of information transport in fiber-optic networks," *Phys. Rev. Lett.*, vol. 101, p. paper 163901, Oct. 2008.
- [41] R.-J. Essiambre, G. Foschini, P. Winzer, and G. Kramer, "Capacity limits of fiber-optic communication systems," in *Opt. Fiber Commun. Conf. (OFC)*, San Diego, CA, USA, Mar. 2009, p. OThL1.
- [42] V. R. Cadambe and S. A. Jafar, "Interference alignment and degrees of freedom of the K -user interference channel," *IEEE Trans. Inf. Theory*, vol. 54, no. 8, pp. 3425–3441, Aug. 2008.
- [43] A. S. Motahari, S. Oveis-Gharan, M. A. Maddah-Ali, and A. K. Khandani, "Real interference alignment: Exploiting the potential of single antenna systems," *IEEE Trans. Inf. Theory*, vol. 60, no. 8, pp. 4799–4810, Aug. 2014.
- [44] M. Abramowitz and I. A. Stegun, *Handbook of Mathematical Functions with Formulas, Graphs, and Mathematical Tables*. New York, 1972.
- [45] I. Gradshteyn and I. Ryzhik, *Table of integrals, series and products*. Academic Press, 2007.
- [46] Y. A. Brychkov, *Handbook of special functions : derivatives, integrals, series and other formulas*, 7th ed. CRC Press, 2008.
- [47] J. G. Proakis and M. Salehi, *Digital Communications*, 5th ed. McGraw-Hill, 2008.
- [48] G. E. Corazza and G. Ferrari, "New bounds for the Marcum Q -function," *IEEE Trans. Inf. Theory*, vol. 48, no. 11, pp. 3003–3008, Nov. 2002.



Hassan Ghazlan (M'15) received the B.S. degree in electrical engineering from Cairo University, Cairo, Egypt, in 2007, the M.S. degree in electrical engineering from Nile University, Cairo, in 2009, and the Ph.D. degree in electrical engineering from the University of Southern California, Los Angeles, CA, USA.

He was a Research Assistant at the Wireless Intelligent Networks Center at Nile University from 2007 to 2009. He was a visiting Ph.D. student at the Technical University of Munich in 2012 and 2013.

He was an intern at Bell Labs in Holmdel, NJ, USA, in 2013. He is currently with Intel Corporation in Hillsboro, OR, USA. His main research interests include communication theory, information theory, and signal processing.



Gerhard Kramer (S'91-M'94-SM'08-F'10) received the Dr. sc. techn. degree from ETH Zurich in 1998. From 1998 to 2000, he was with Endora Tech AG in Basel, Switzerland, and from 2000 to 2008 he was with the Math Center at Bell Labs in Murray Hill, NJ, USA. He joined the University of Southern California, Los Angeles, CA, USA, as a Professor of Electrical Engineering in 2009. He joined the Technical University of Munich (TUM) in 2010, where he is currently Alexander von Humboldt Professor and Chair for Communications Engineering.

His research interests include information theory and communications theory, with applications to wireless, copper, and optical fiber networks. Dr. Kramer served as the 2013 President of the IEEE Information Theory Society. He was elected to the Bavarian Academy of Sciences and Humanities in 2015.